Calorimetric Electron Telescope (CALET): Summary of the First Two-Years on Orbit

Shoji Torii
for the CALET collaboration
Waseda University

International Symposium on Cosmology and Particle Astrophysics

CosPA 2017

December 11-15, 2017
Yukawa Institute for Theoretical Physics, Kyoto University, JAPAN

CALET collaboration team

O. Adriani[25], Y. Akaike[2], K. Asano[7], Y. Asaoka[9,31], M.G. Bagliesi[29], G. Bigongiari[29], W.R. Binns[32], S. Bonechi[29], M. Bongi[25], P. Brogi[29], J.H. Buckley[32], N. Cannady[12], G. Castellini[25], C. Checchia[26], M.L. Cherry[12], G. Collazuol[26], V. Di Felice[28], K. Ebisawa[8], H. Fuke[8], G.A. de Nalfo [14], T.G. Guzik[12], T. Hams[3], M. Hareyama[23], N. Hasebe[31], K. Hibino[10], M. Ichimura[4], K. Ioka[34], W.Ishizaki[7], M.H. Israel[32], A. Javaid[12], K. Kasahara[31], J. Kataoka[31], R. Kataoka[16], Y. Katayose[33], C. Kato[22], Y.Kawakubo[1], N. Kawanaka[30], H. Kitamura[15], H.S. Krawczynski[32], J.F. Krizmanic[2], S. Kuramata[4], T. Lomtadze[27], P. Maestro[29], P.S. Marrocchesi[29], A.M. Messineo[27], J.W. Mitchell[14], S. Miyake[5], K. Mizutani[20], A.A. Moiseev[3], K. Mori[9,31], M. Mori[19], N. Mori[25], H.M. Motz[31], K. Munakata[22], H. Murakami[31], Y.E. Nakagawa[8], S. Nakahira[9], J. Nishimura[8], S. Okuno[10], J.F. Ormes[24], S. Ozawa[31], L. Pacini[25], F. Palma[28], P. Papini[25], A.V. Penacchioni[29], B.F. Rauch[32], S.B. Ricciarini[25], K. Sakai[3], T. Sakamoto[1], M. Sasaki[3], Y. Shimizu[10], A. Shiomi[17], R. Sparvoli[28], P. Spillantini[25], F. Stolzi[29], I. Takahashi[11], M. Takayanagi[8], M. Takita[7], T. Tamura[10], N. Tateyama[10], T. Terasawa[7], H. Tomida[8], S. Torii[9,31], Y. Tunesada[18], Y. Uchihori[15], S. Ueno[8], E. Vannuccini[25], J.P. Wefel[12], K. Yamaoka[13], S. Yanagita[6], A. Yoshida[1], K. Yoshida[21], and T. Yuda[7]

1) Aoyama Gakuin University, Japan
2) CRESST/NASA/GSFC and Universities Space Research Association, USA
3) CRESST/NASA/GSFC and University of Maryland, USA
4) Hirosaki University, Japan
5) Ibaraki National College of Technology, Japan
6) Ibaraki University, Japan
7) ICRR, University of Tokyo, Japan
8) ISAS/JAXA Japan
9) JAXA, Japan
10) Kanagawa University, Japan
11) Kavli IPMU, University of Tokyo, Japan
12) Louisiana State University, USA
13) Nagoya University, Japan
14) NASA/GSFC, USA
15) National Inst. of Radiological Sciences, Japan
16) National Institute of Polar Research, Japan
17) Nihon University, Japan
18) Osaka City University, Japan
19) Ritsumeikan University, Japan
20) Saitama University, Japan
21) Shibaura Institute of Technology, Japan
22) Shinshu University, Japan
23) St. Marianna University School of Medicine, Japan
24) University of Denver, USA
25) University of Florence, IFAC (CNR) and INFN, Italy
26) University of Padova and INFN, Italy
27) University of Pisa and INFN, Italy
28) University of Rome Tor Vergata and INFN, Italy
29) University of Siena and INFN, Italy
30) University of Tokyo, Japan
31) Waseda University, Japan
32) Washington University-St. Louis, USA
33) Yokohama National University, Japan
34) Yukawa Institute for Theoretical Physics, Kyoto University, Japan

CALET collaboration team

O. Adriani[25], Y. Akaike[2], K. Asano[7], Y. Asaoka[9,31], M.G. Bagliesi[29], G. Bigongiari[29], W.R. Binns[32], S. Bonechi[29], M. Bongi[25], P. Brogi[29], J.H. Buckley[32], N. Cannady[12], G. Castellini[25], C. Checchia[26], M.L. Cherry[12], G. Collazuol[26], V. Di Felice[28], K. Ebisawa[8], H. Fuke[8], G.A. de Nalfo [14], T.G. Guzik[12], T. Hams[3], M. Hareyama[23], N. Hasebe[31], K. Hibino[10], M. Ichimura[4], K. Ioka[34], W.Ishizaki[7], M.H. Israel[32], A. Javaid[12], K. Kasahara[31], J. Kataoka[31], R. Kataoka[16], Y. Katayose[33], C. Kato[22], Y.Kawakubo[1], N. Kawanaka[30], H. Kitamura[15], H.S. Krawczynski[32], J.F. Krizmanic[2], S. Kuramata[4], T. Lomtadze[27], P. Maestro[29], P.S. Marrocchesi[29], A.M. Messineo[27], J.W. Mitchell[14], S. Miyake[5], K. Mizutani[20], A.A. Moiseev[3], K. Mori[9,31], M. Mori[19], N. Mori[25], H.M. Motz[31], K. Munakata[22], H. Murakami[31], Y.E. Nakagawa[8], S. Nakahira[9], J. Nishimura[8], S. Okuno[10], J.F. Ormes[24], S. Ozawa[31], L. Pacini[25], F. Palma[28], P. Papini[25], A.V. Penacchioni[29], B.F. Rauch[32], S.B. Ricciarini[25], K. Sakai[3], T. Sakamoto[1], M. Sasaki[3], Y. Shimizu[10], A. Shiomi[17], R. Sparvoli[28], P. Spillantini[25], F. Stolzi[29], I. Takahashi[11], M. Takayanagi[8], M. Takita[7], T. Tamura[10], N. Tateyama[10], T. Terasawa[7], H. Tomida[8], S. Torii[9,31], Y. Tunesada[18], Y. Uchihori[15], S. Ueno[8], E. Vannuccini[25], J.P. Wefel[12], K. Yamaoka[13], S. Yanagita[6], A. Yoshida[1], K. Yoshida[21], and T. Yuda[7]

CALET Payload

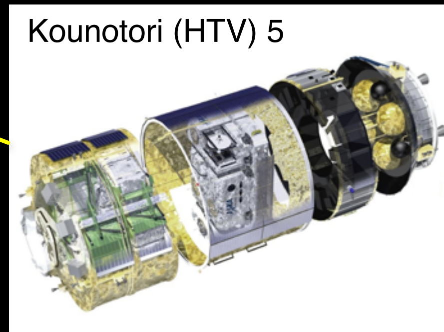

Launched on Aug. 19th, 2015 by the Japanese H2-B rocket

Emplaced on JEM-EF port #9 on Aug. 25th, 2015 (JEM-EF: Japanese Experiment Module-Exposed Facility)

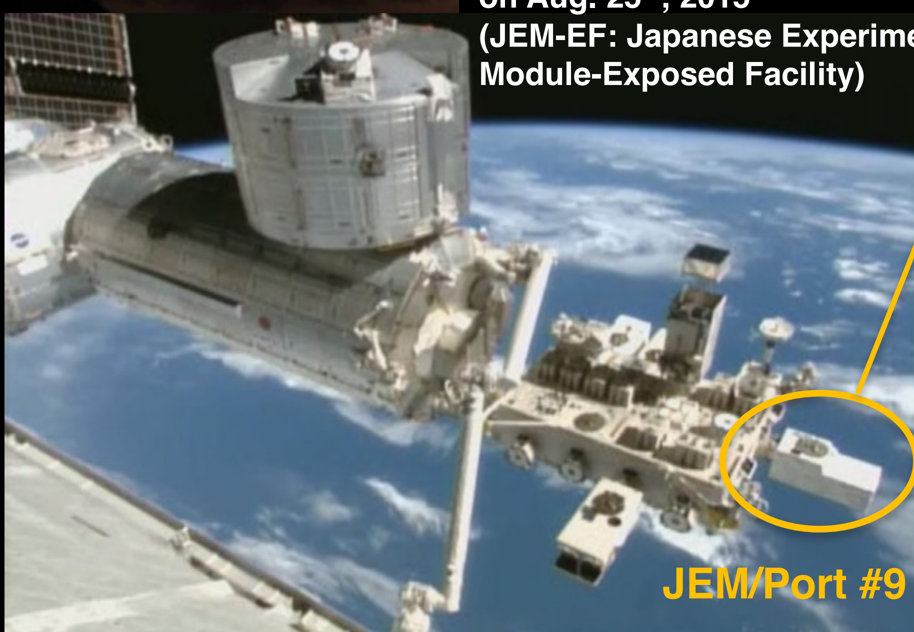

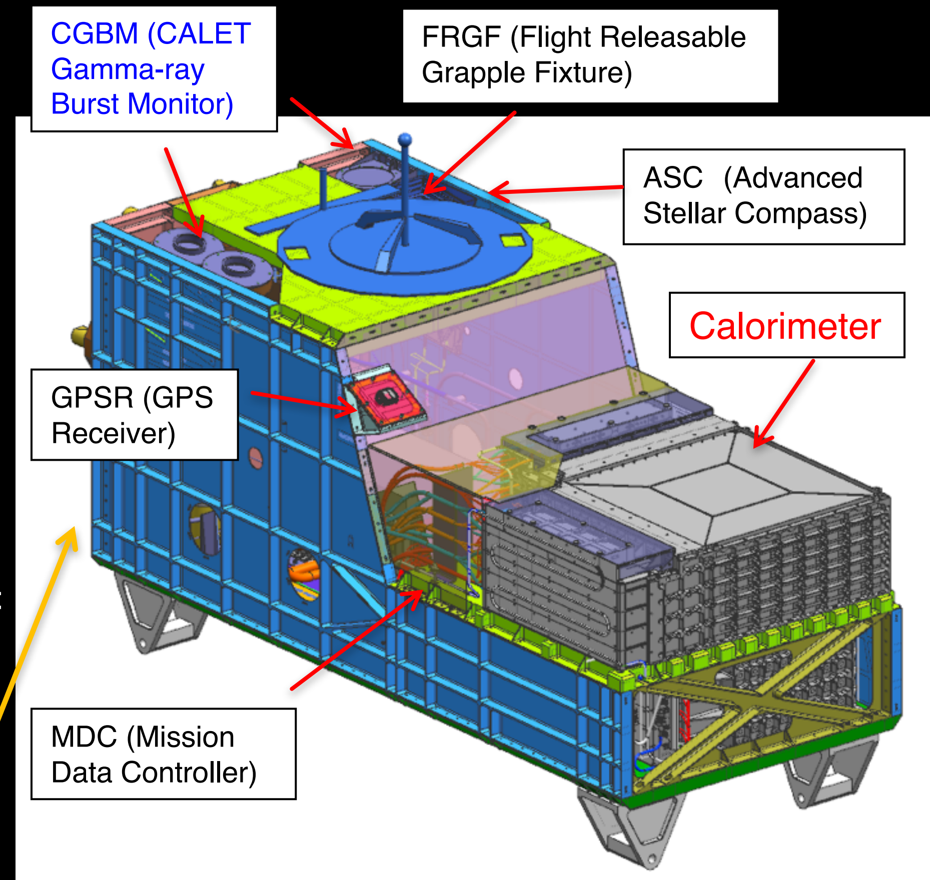

- **Mass: 612.8 kg**
- **JEM Standard Payload Size:**
  1850mm(L) × 800mm(W) × 1000mm(H)
- **Power Consumption: 507 W (max)**
- **Telemetry:**
  Medium 600 kbps (6.5GB/day) / Low 50 kbps

CALET Instrument

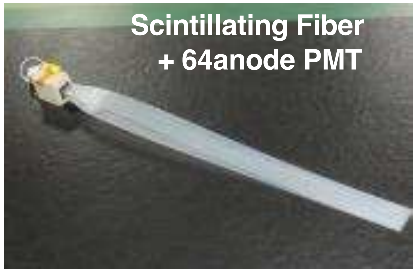

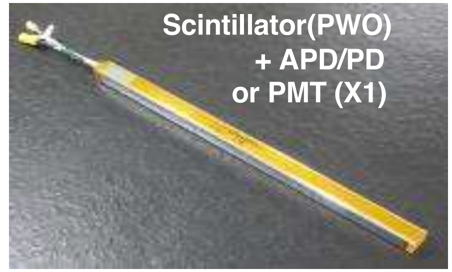

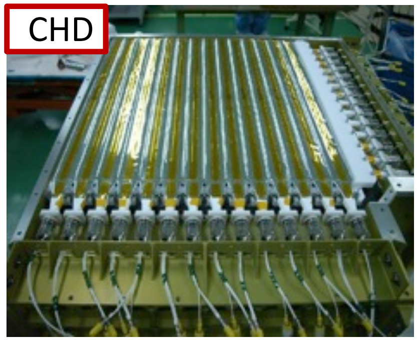

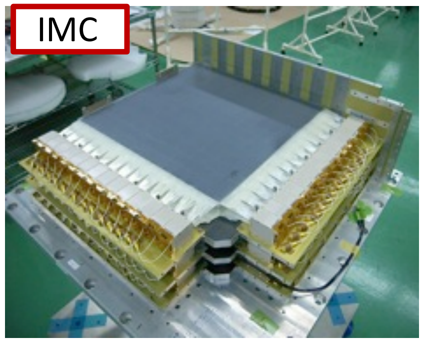

CALORIMETER

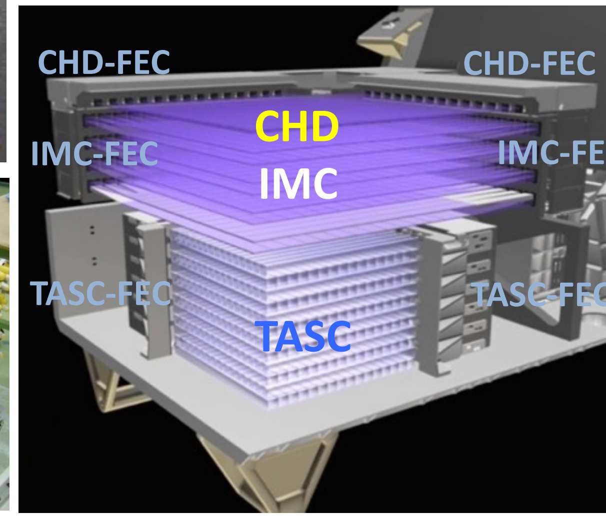

	CHD (Charge Detector)	IMC (Imaging Calorimeter)	TASC (Total Absorption Calorimeter)
Measure	Charge (Z=1-40)	Tracking , Particle ID	Energy, e/p Separation
Geometry (Material)	Plastic Scintillator 14 paddles x 2 layers (X,Y): 28 paddles Paddle Size: 32 x 10 x 450 mm^3	448 Scifi x 16 layers (X,Y) : 7168 Scifi 7 W layers ($3X_0$): $0.2X_0$ x 5 + $1X_0$ x2 Scifi size : 1 x 1 x 448 mm^3	16 PWO logs x 12 layers (x,y): 192 logs log size: 19 x 20 x 326 mm^3 Total Thickness : 27 X_0 , ~1.2 λ_I
Readout	PMT+CSA	64-anode PMT+ ASIC	APD/PD+CSA PMT+CSA (for Trigger)@top layer

CALET Capability

Field of view: ~ 45 degrees (from the zenith)
Geometrical Factor: ~ 1,040 cm^2sr (for electrons)

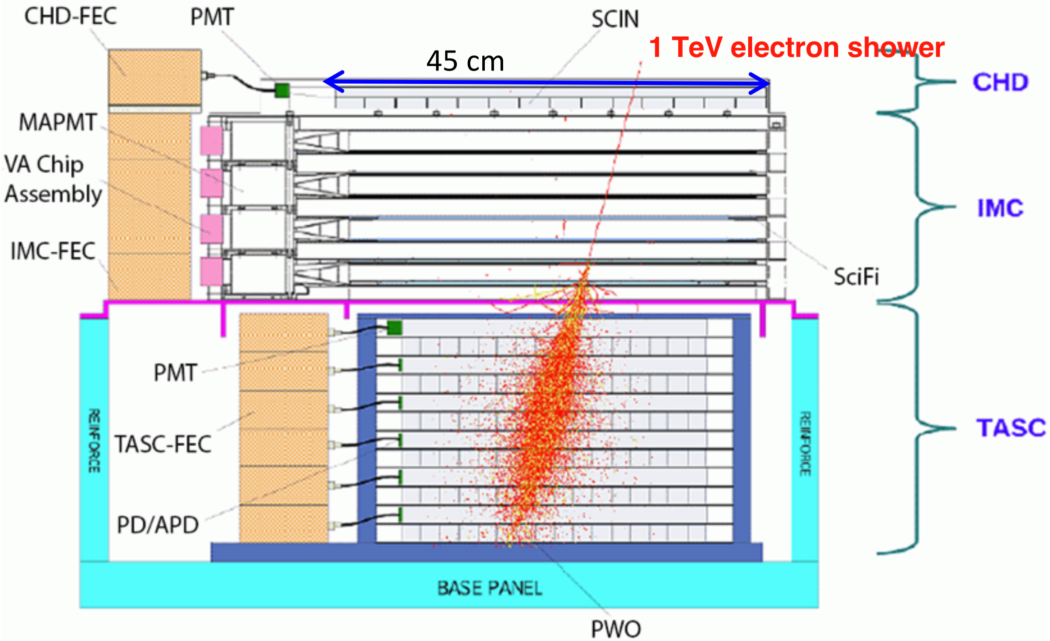

Unique features of CALET

- **A dedicated charge detector + multiple dE/dx track sampling in the IMC allow to identify individual nuclear species (Δz~0.15-0.3 e).**
- **Thick(~30 X_0), fully active calorimeter allows measurements well into the TeV energy region with excellent energy resolution (~2-3%)**
- **High granularity imaging pre-shower calorimeter accurately identify the arrival direction of incident particles (~0.2°) and the starting point of electro-magnetic showers.**
- **Combined, they powerfully separate electrons from the abundant protons: contamination is much less than 10 % up to the TeV region.**

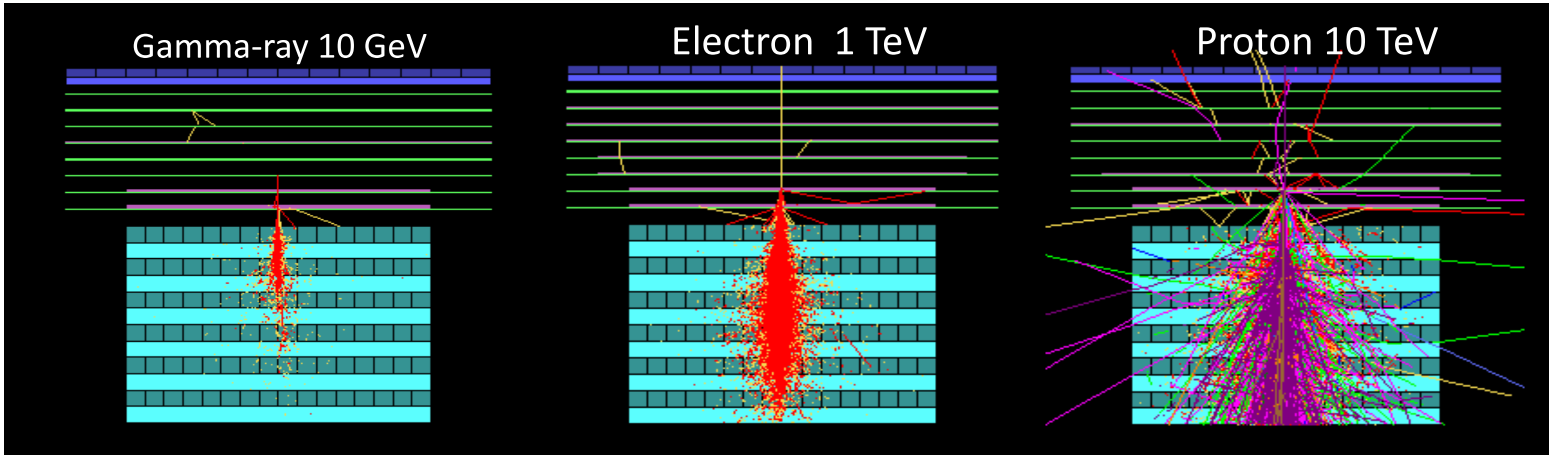

Scientific Targets

Scientific Objectives	Observation Targets	Energy Range
CR Origin and Acceleration	Electron spectrum p--Fe individual spectra Ultra Heavy Ions (26<Z≤40) Gamma-rays (Diffuse + Point sources)	1GeV - 20 TeV 10 GeV - 1000 TeV > 600 MeV/n 1 GeV - 1 TeV
Galactic CR Propagation	B/C and sub-Fe/Fe ratios	Up to some TeV/n
Nearby CR Sources	Electron spectrum	100 GeV - 20 TeV
Dark Matter	Signatures in electron/gamma-ray spectra	100 GeV - 20 TeV
Solar Physics	Electron flux	< 10 GeV
Gamma-ray Transients	Gamma-rays and X-rays	7 keV - 20 MeV

Scientific Targets

Scientific Objectives	Observation Targets	Energy Range
CR Origin and Acceleration	Electron spectrum p--Fe individual spectra Ultra Heavy Ions (26<Z≤40) Gamma-rays (Diffuse + Point sources)	1GeV - 20 TeV 10 GeV - 1000 TeV > 600 MeV/n 1 GeV - 1 TeV
Galactic CR Propagation	B/C and sub-Fe/Fe ratios	Up to some TeV/n
Nearby CR Sources	Electron spectrum	100 GeV - 20 TeV
Dark Matter	Signatures in electron/gamma-ray spectra	100 GeV - 20 TeV
Solar Physics	Electron flux	< 10 GeV
Gamma-ray Transients	Gamma-rays and X-rays	7 keV - 20 MeV

Respond to the unresolved questions from the results found by recent observations

Increase of positron/electron ratio

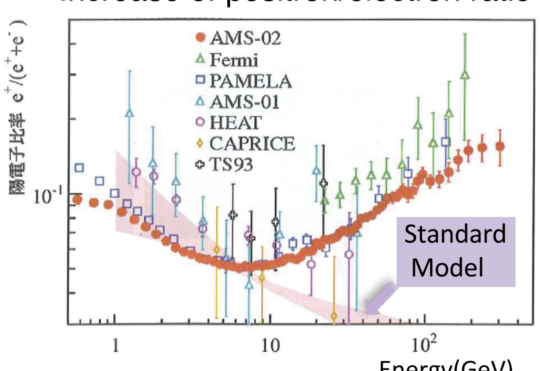

Excess of electron+positron flux

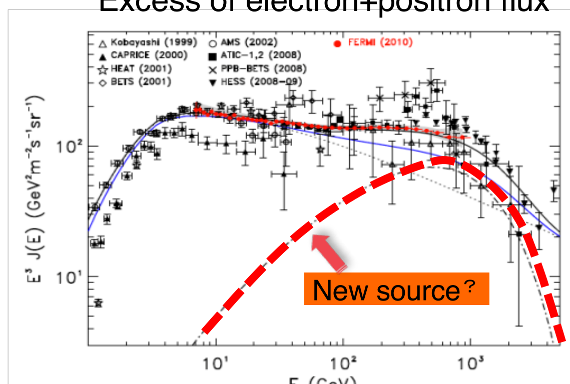

Hardening of p, He spectra

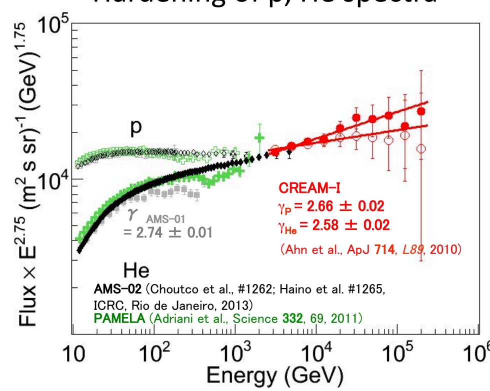

New source of electrons and positrons at 100 GeV ?

CALET Main Target: Identification of Electron Sources

Some nearby sources, e.g. Vela SNR, is likely to have unique signatures in the electron energy spectrum in the TeV region (Kobayashi et al. ApJ 2004)

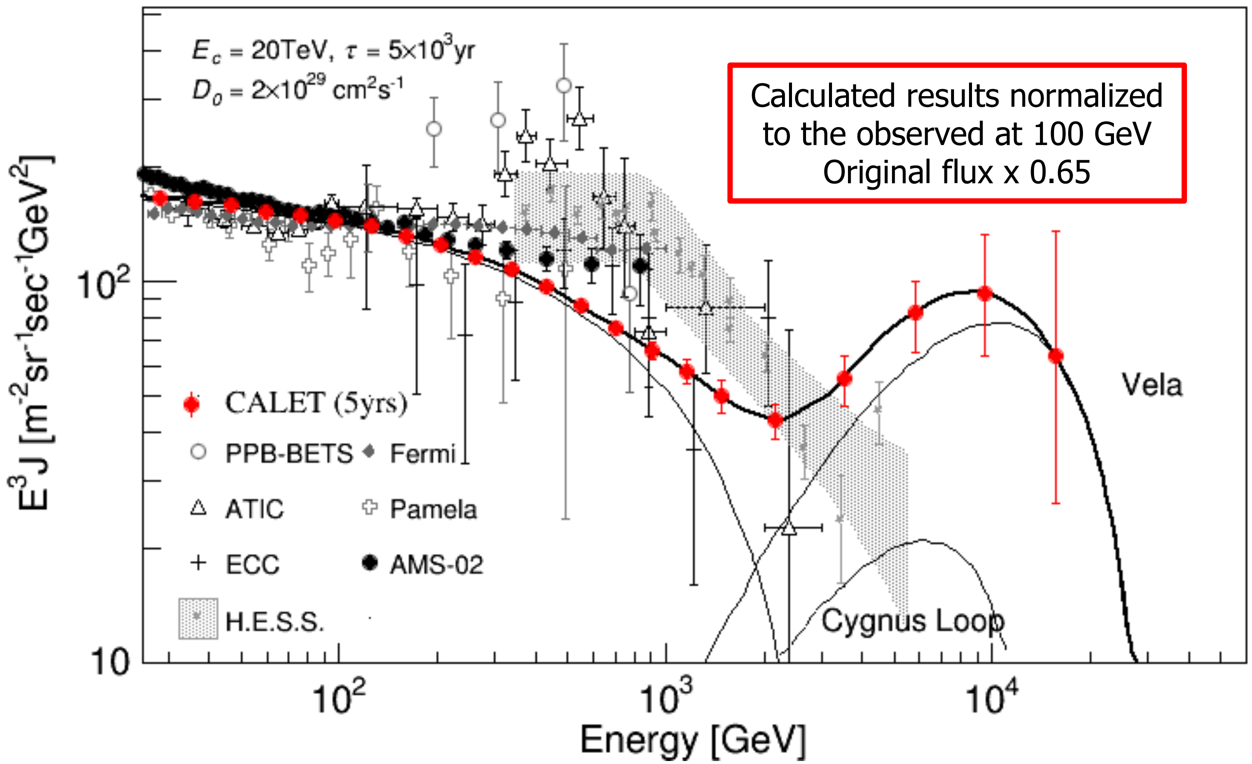

Expected Anisotropy from Vela

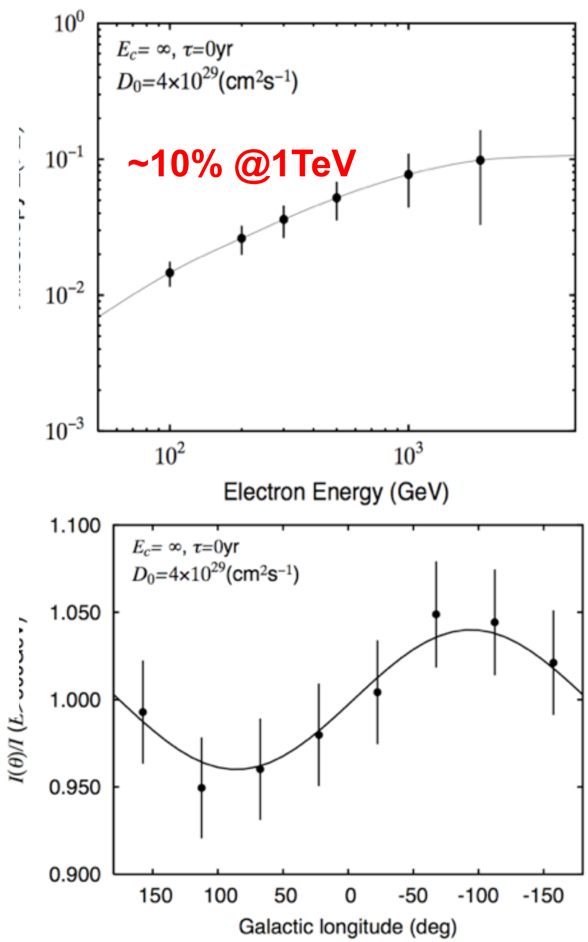

▶ Identification of the unique signature from nearby SRNs, such as Vela, in the electron spectrum by CALET in the TeV region

CALET Main Target: Identification of Electron Sources

Some nearby sources, e.g. Vela SNR, is likely to have unique signatures in the electron energy spectrum in the TeV region (Kobayashi et al. ApJ 2004)

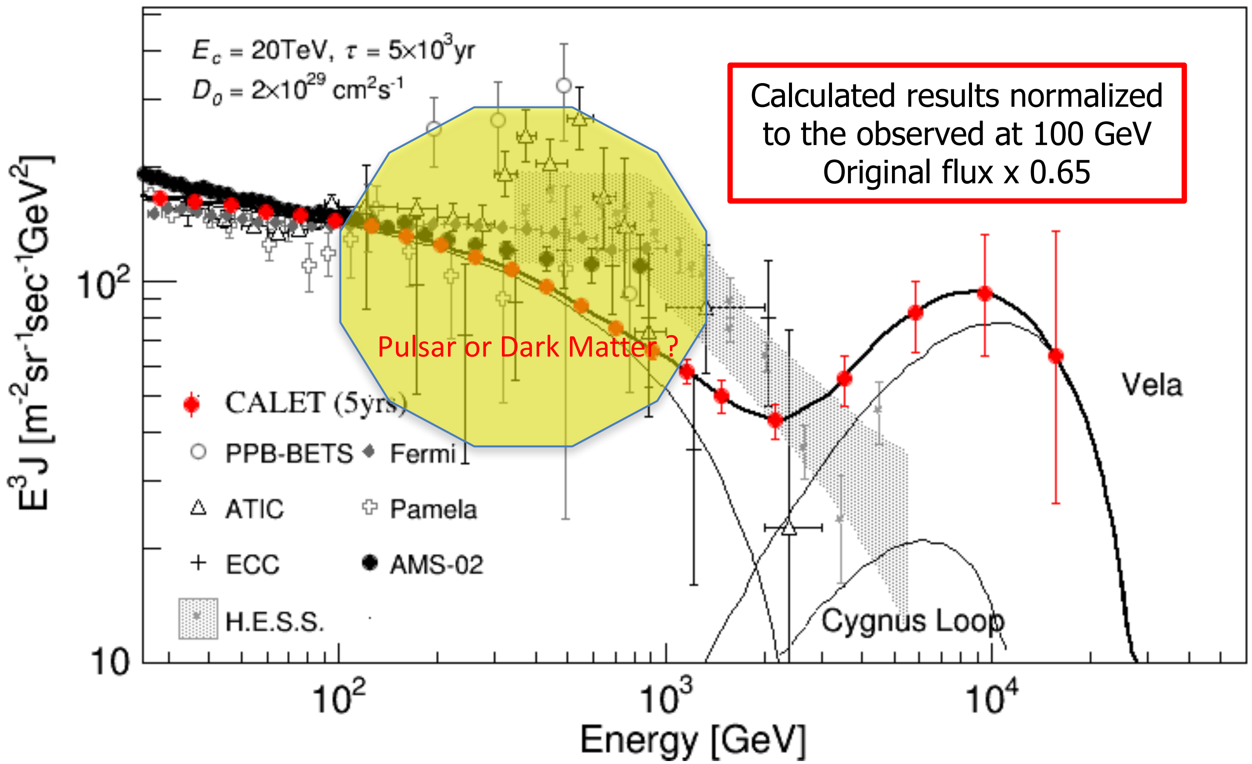

Expected Anisotropy from Vela

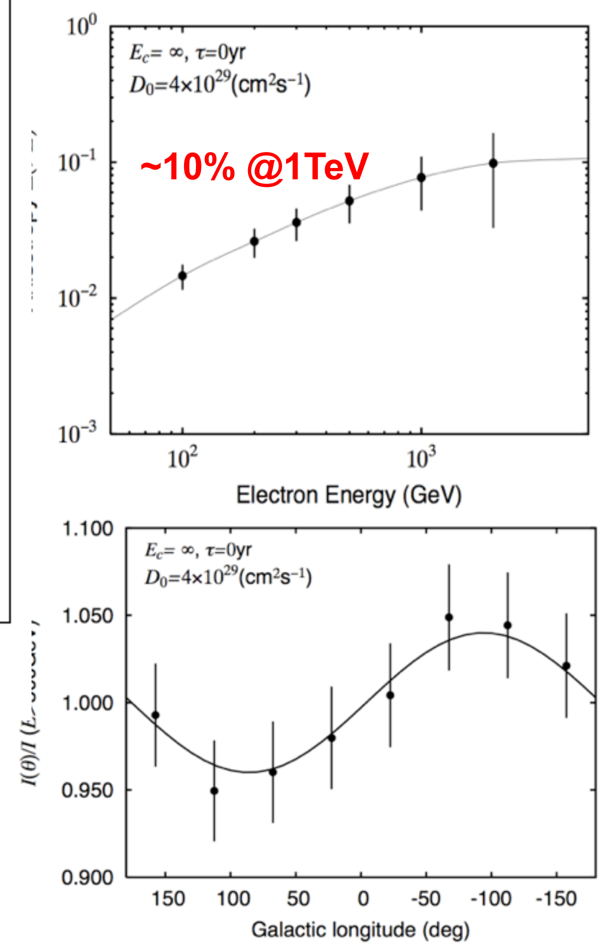

▶ Identification of the unique signature from nearby SRNs, such as Vela, in the electron spectrum by CALET in the TeV region

Measurements of Cosmic-Ray Nuclei Spectra with CALET

- Hardening in the p and He at 200 GV observed by PAMELA
- p and He spectra have different slopes in the multi TeV region (CREAM)
- Acceleration limit by SNR shock wave around 100 TeV/Z ?

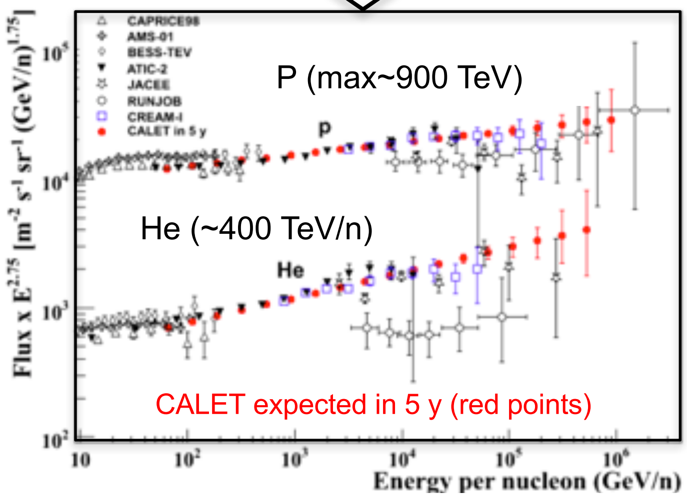

- All primary heavy nuclei spectra well fitted to single power-laws with similar spectral index (CREAM, TRACER)
- However hint of a hardening from a combined fit to all nuclei spectra (CREAM)

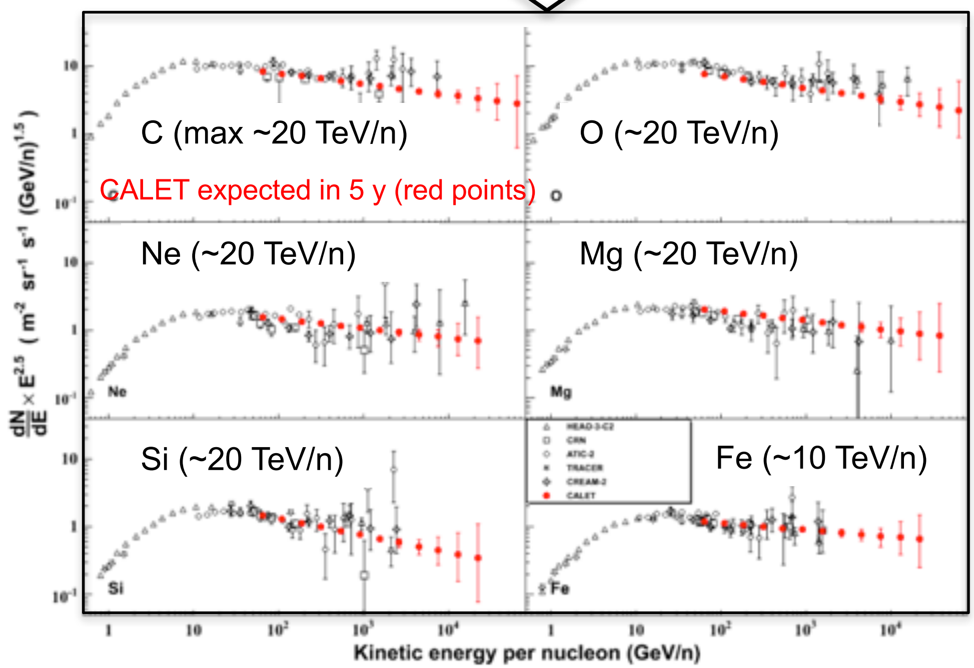

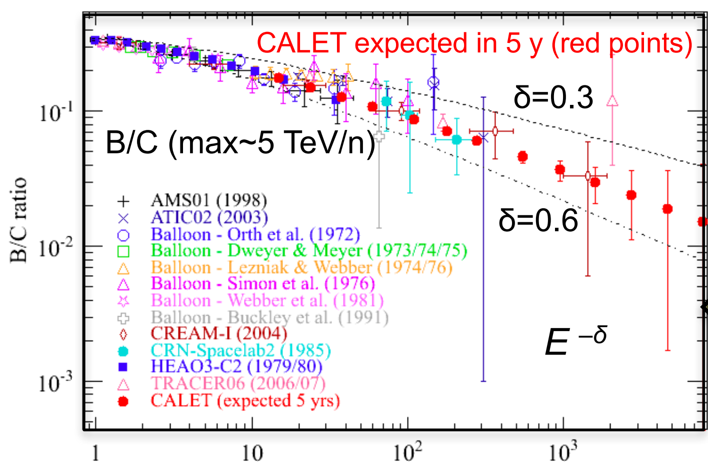

- At high energy (> 10 GeV/n) the B/C ratio measures the energy dependence of the escape path-length, $\sim E^{-\delta}$, of CRs from the Galaxy
- Data around 100 GeV/n indicate δ~0.6. At highest energy the ratio is expected to flatten out.

Observation by High Energy Trigger (>10GeV)

Observation by High Energy Trigger for 780 days : Oct.13, 2015 – Nov.30, 2017

- The exposure, SΩT, has reached to ~68.1 m^2 sr day for electron observations by continuous and stable operations.
- Total number of the triggered events is ~ 508 million with a live time fraction of 84.0 %.

Accumulated observation time (live, dead)

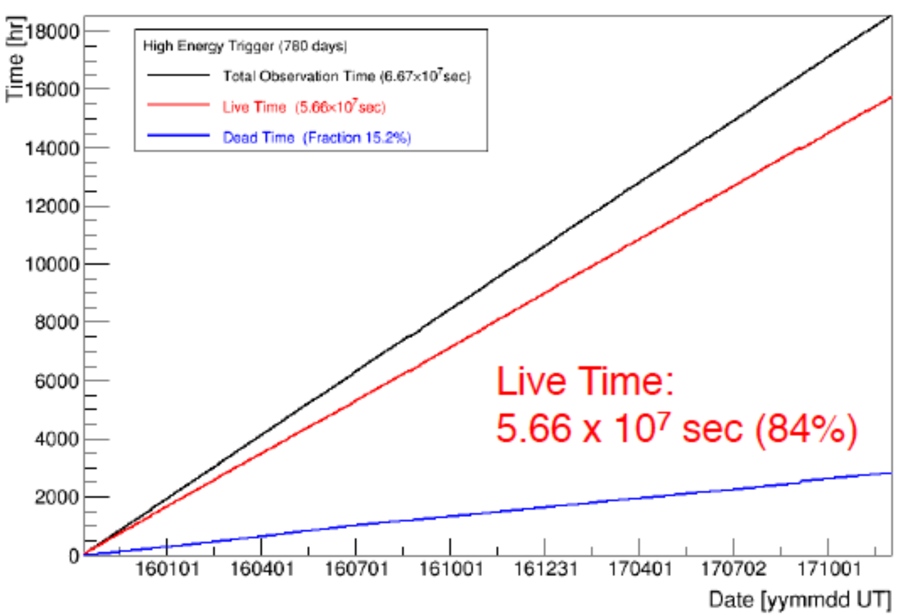

Accumulated triggered event number

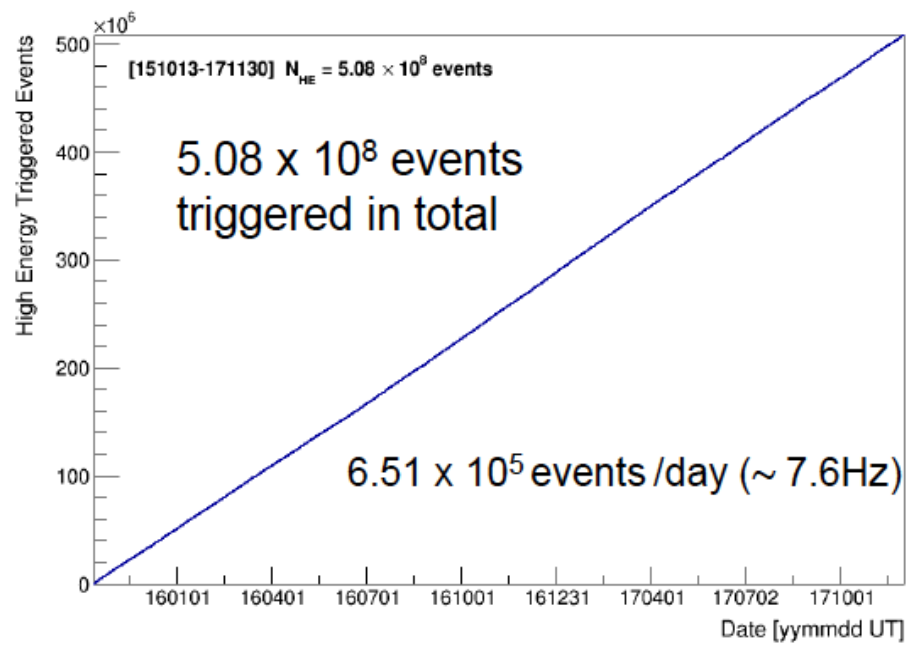

Energy Reconstruction for Electromagnetic Showers

Simulation: Comparison of deposit energy in TASC (ΔE) with incident energy (E_0)

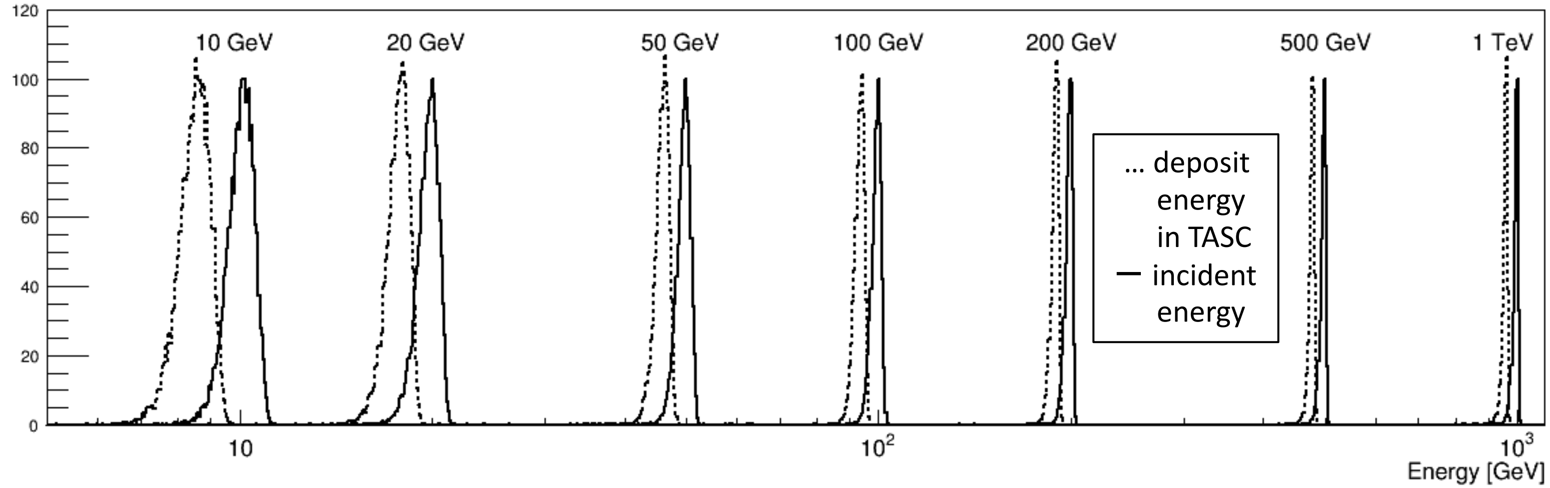

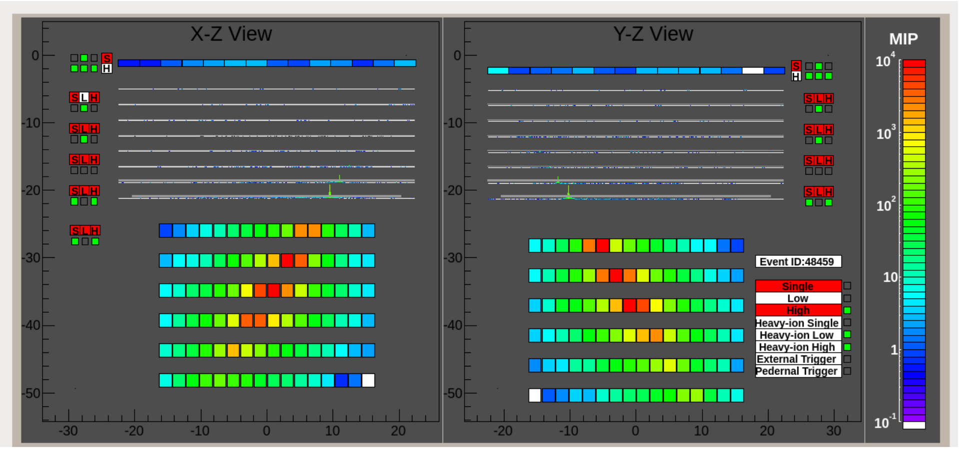

4 TeV electron candidate (well contained)
⇒ very small leakage (~ a few %)

Energy reconstruction factor vs. Energy

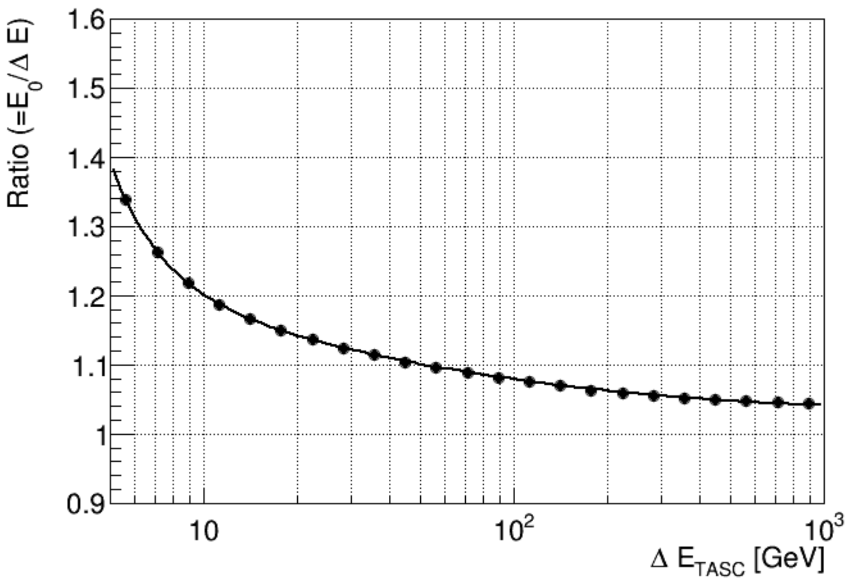

Energy Reconstruction for Electromagnetic Showers

(A) Fully-contained (B) Nearly fully-contained (C) Side-incident (D) Side-out

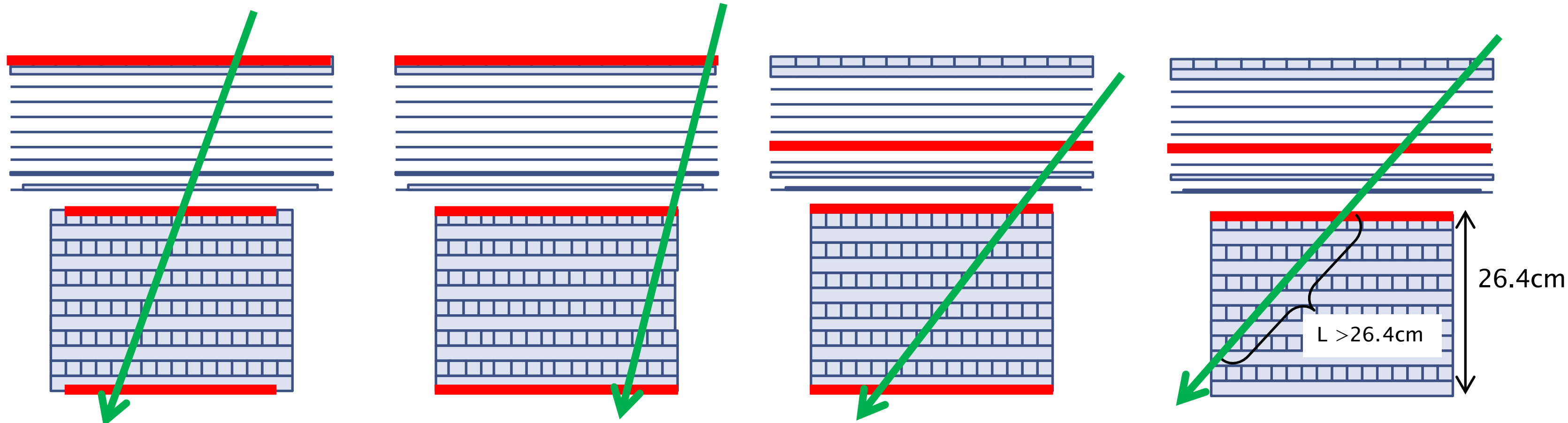

SΩ (cm^2sr) 416 A+B:570 All: 1040

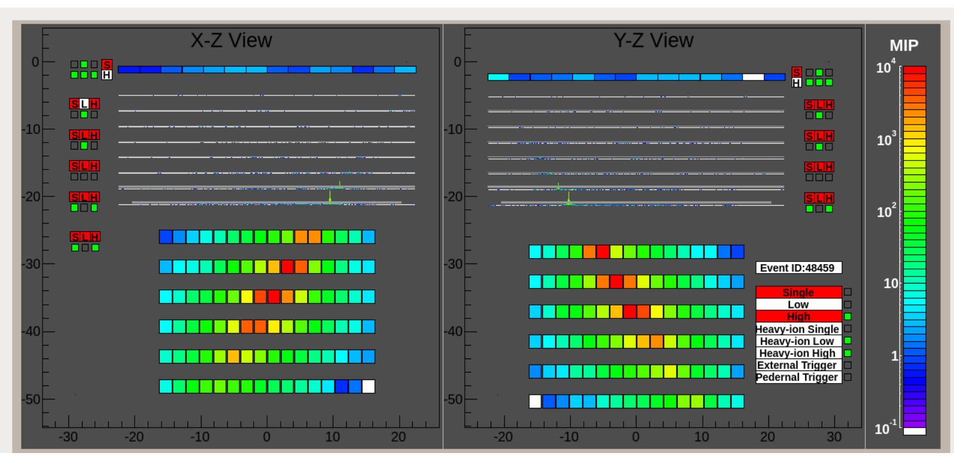

4 TeV electron candidate (well contained)
⇒ very small leakage (~ a few %)

Energy reconstruction factor vs. Energy

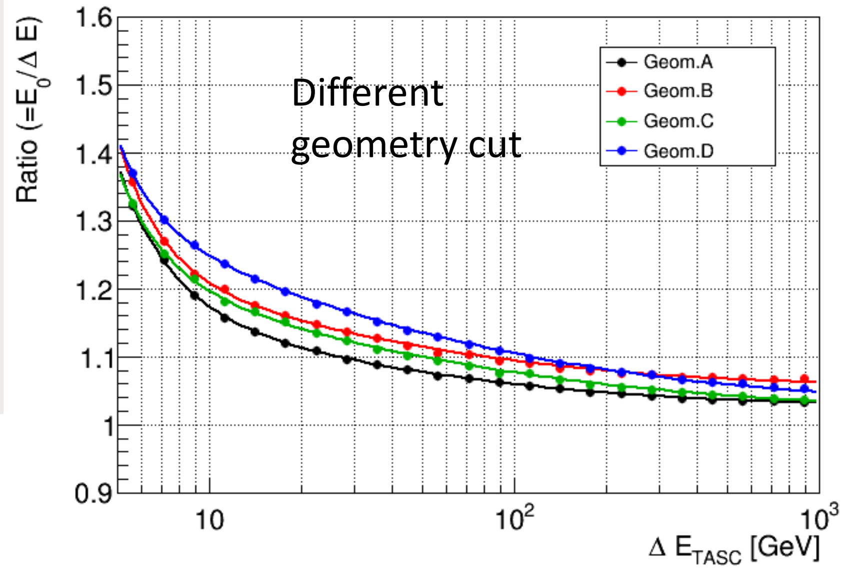

Position and Temperature Calibration, and Long-term Stability

Example of position dependence correction

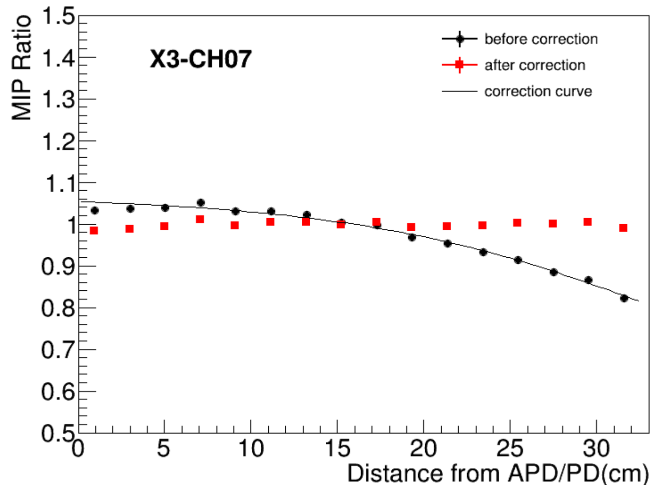

Examples of temperature change correction

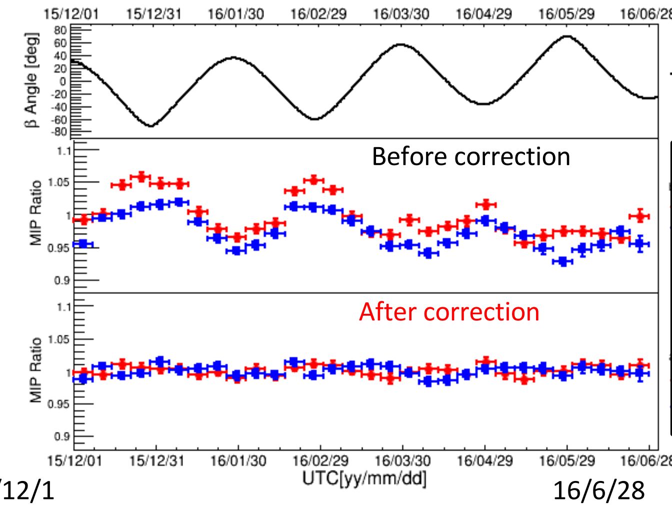

Active Thermal Control System (ATCS) on ISS can provide very stable thermal condition during Long-tem observations: Δt ~ a few degrees

Example of long-term variation correction

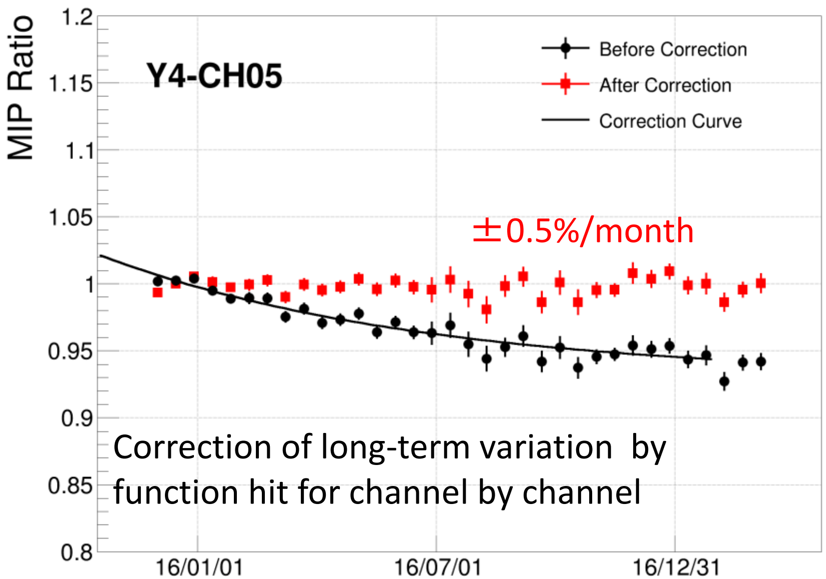

Distribution of MIPs for 192 ch x 16 segmented positions after each correction

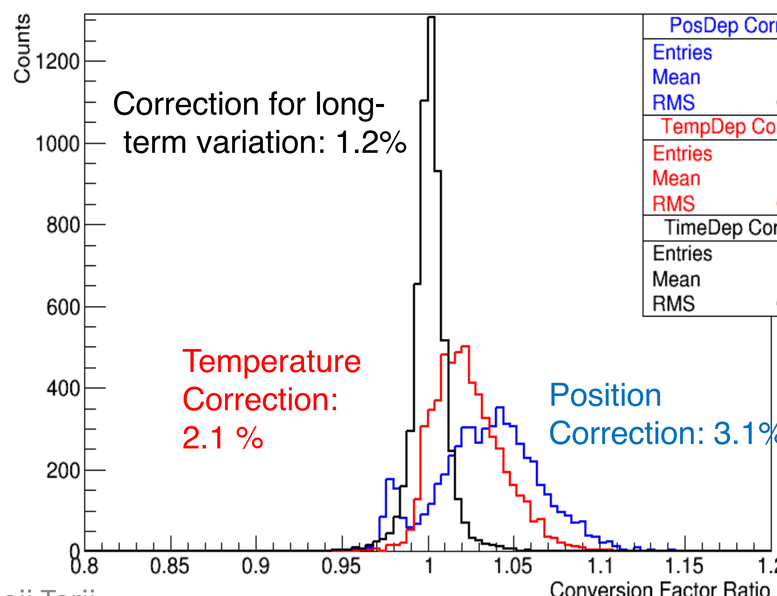

Energy Measurement in Dynamic Range of 1-10^6 MIP in TASC

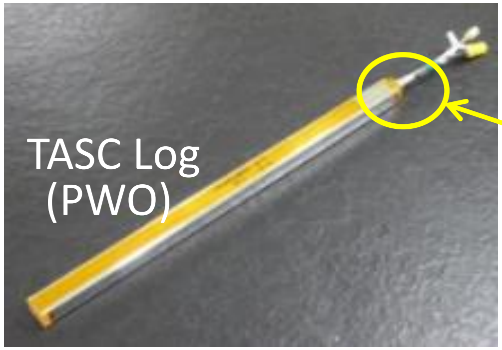

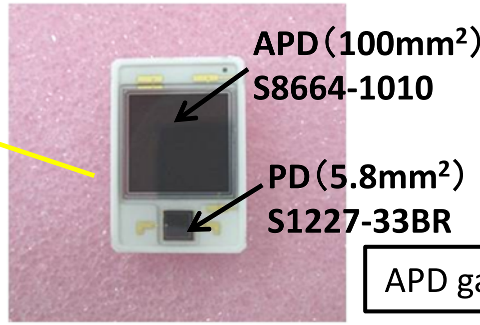

APD gain ~50

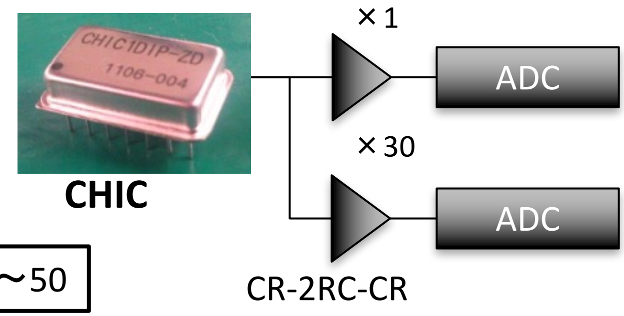

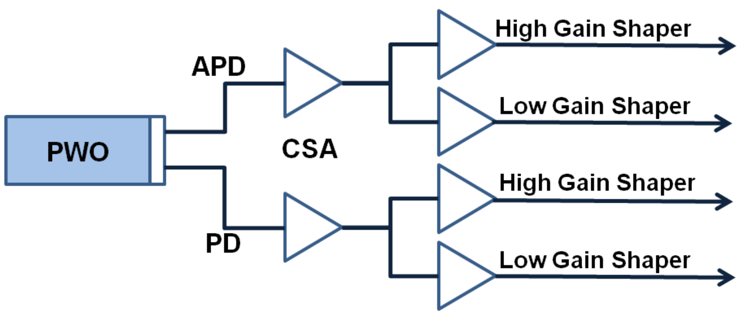

The linearity was calibrated by using UV laser irradiation on ground :

1) The linearity is confirmed in the range of 1.4-2.5 %.
2) The whole dynamic range is confirmed to cover from 1 MIP to 10^6 MIPs.

APD-H	APD-L	PD-H	PD-L
1.4%	1.5%	2.5%	2.2%

The correlation between adjacent gain ranges is calibrated by using in-flight data in each channel.

APD-H APD-L	APD-L PD-H	PD-H PD-L
0.1%	0.7%	0.1%

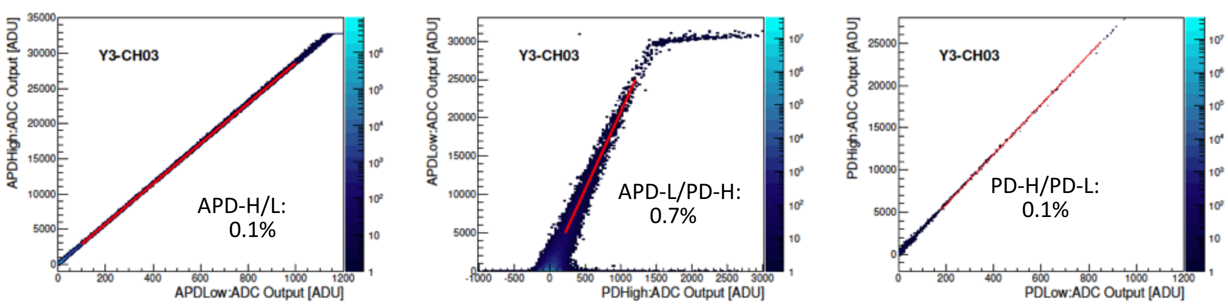

Example of energy distribution in one PWO log

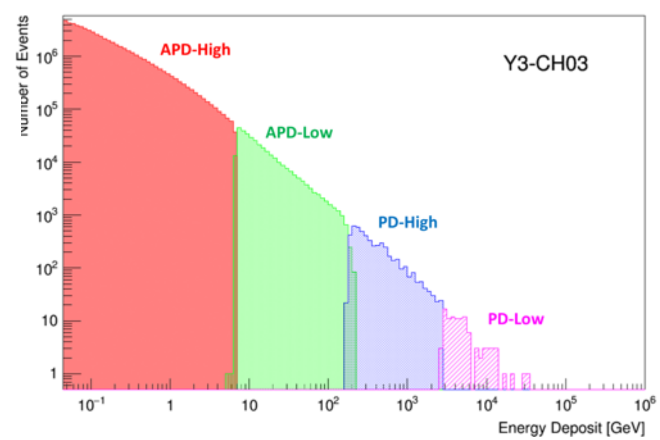

Energy Resolution for Electrons by On-orbit Calibration

Y.Asaoka, Y.Akaike, Y.Komiya, R.Miyata, S.Torii et al.,
Astroparticle Physics 91 (2017) 1.

Considering the calibration errors and instrument noise, energy resolution is estimated as a function of energy.

Energy dependence of energy resolution

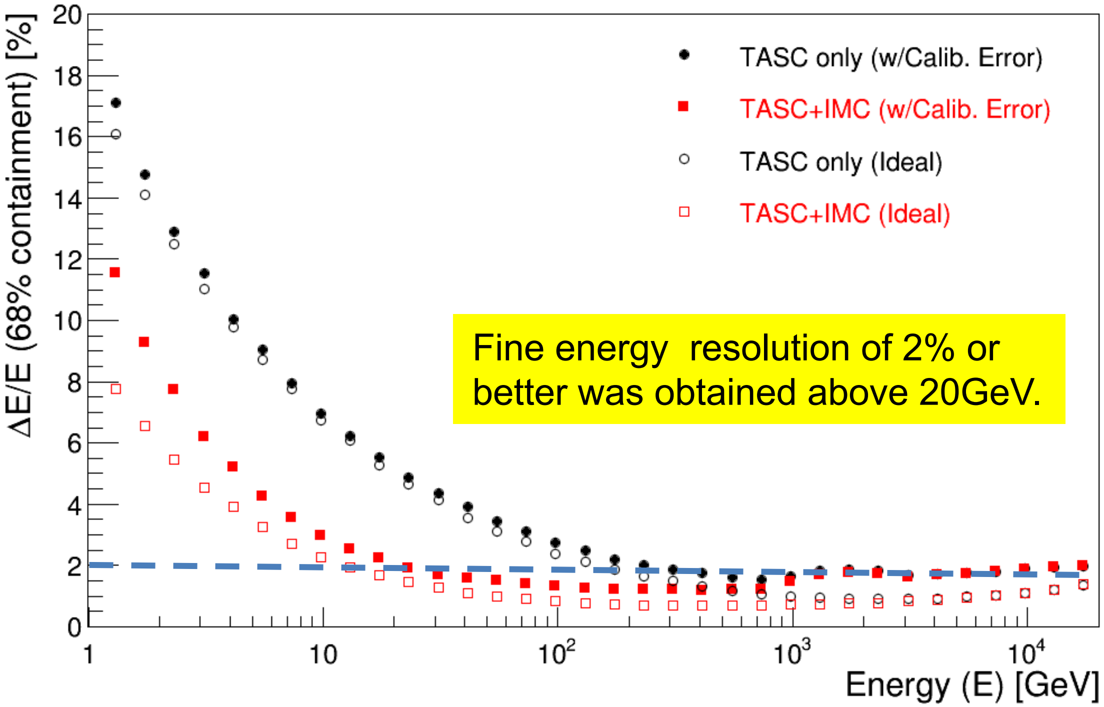

Error budget in energy calibration

MIP	Energy conversion	2.6%
	Peak fitting of MC and flight data	0.6%
	Fitting range dependence	0.6%(*)
	Position dependence	1.8%
	Temperature dependence	1.0%
	Rigidity cutoff dependence	1.0%(*)
	Systematic uncertainty estimated from p/He consistency	1.0%
UV Laser	Linearity	1.4~2.5%
	Fit error	
	APD high gain	1.4%
	APD low gain	1.5%
	PD high gain	2.5%
	PD low gain	2.2%
Gain Ratio	Gain range connection	1.6~2.1%
	Fit error	
	APD-high to APD-low gain	0.1%
	APD-low to PD-high gain	0.7%
	PD high to PD low gain	0.1%
	Slope extrapolation	
	APD-high to APD-low gain	1.6%
	APD-low to PD-high gain	2.0%(*)
	PD high to PD low gain	1.8%
Sampling Bias		0.5%(**)

(*) also considered as systematic error on energy scale
(**) energy-scale systematic error only

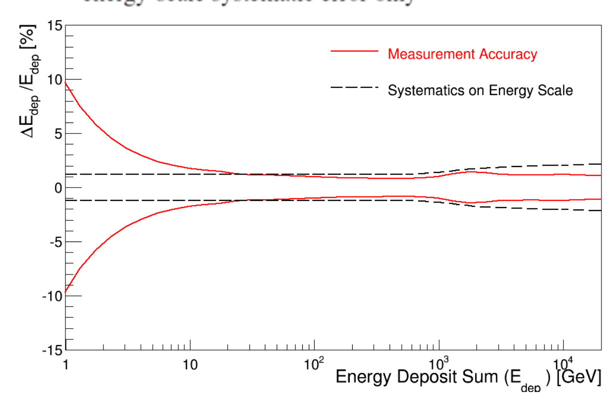

Energy Deposit Distribution of All Triggered-Events by Observation for 780 days

Distribution of deposit energies in TASC observed in 2015.10.13—2017.11.30

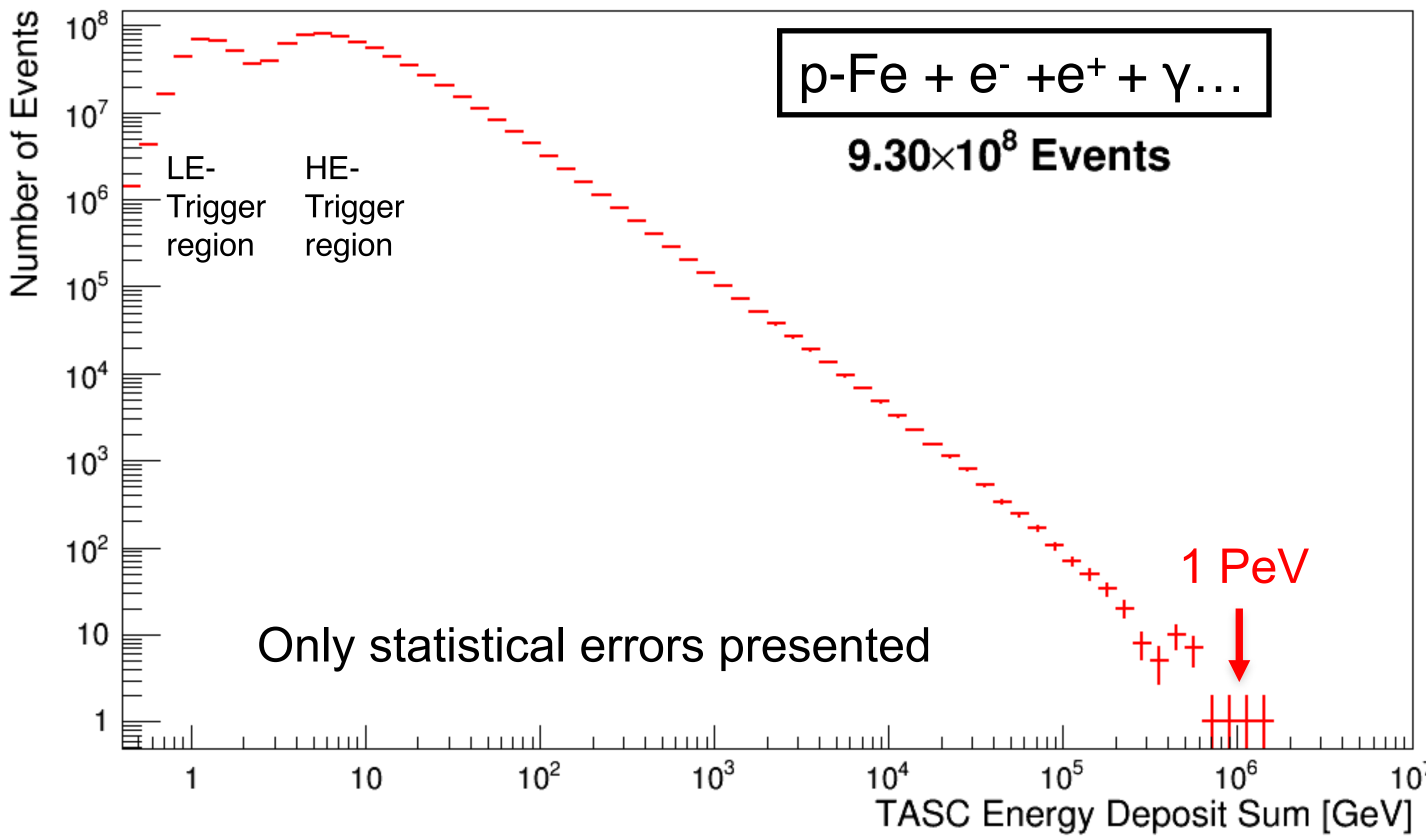

➡ Energies are calibrated but non-reconstructed

The TASC energy measurements have successfully been carried out in the dynamic range of 1 GeV – 1 PeV.

Examples of Event Display

Electron, E=3.05 TeV

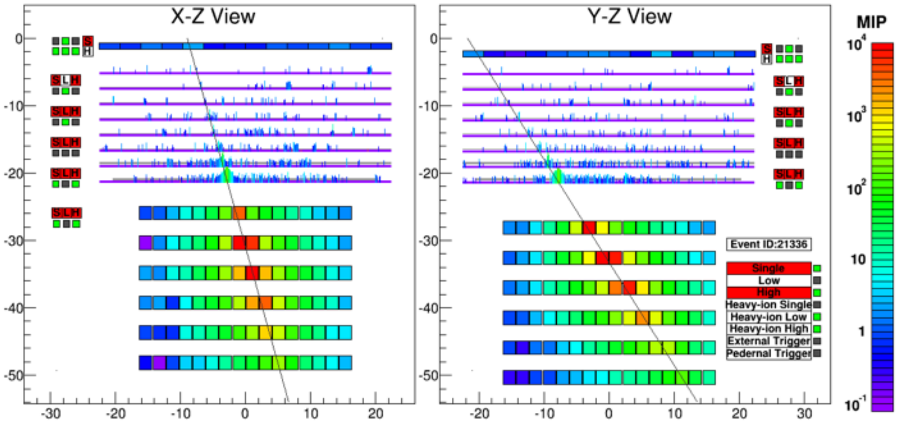

Proton, ΔE=2.89 TeV

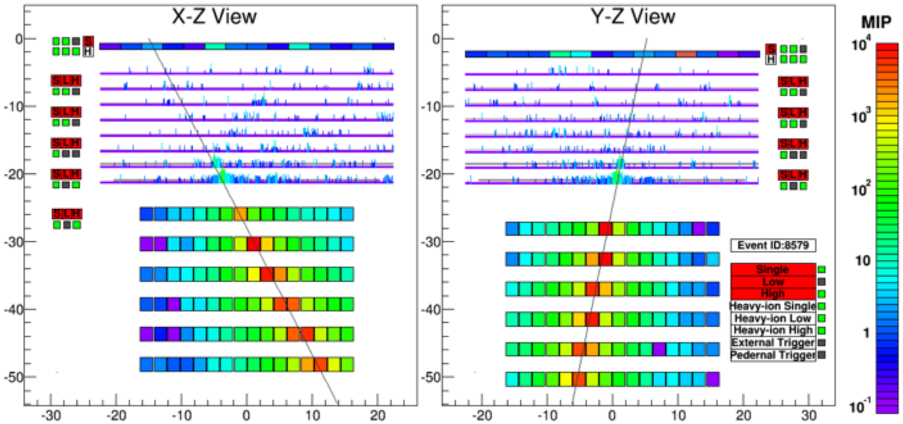

Fe, ΔE=9.3 TeV

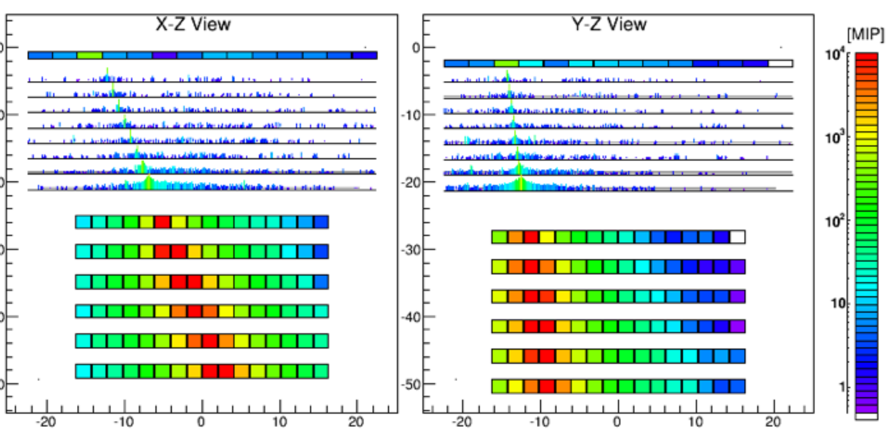

Gamma-ray, E=44.3 GeV

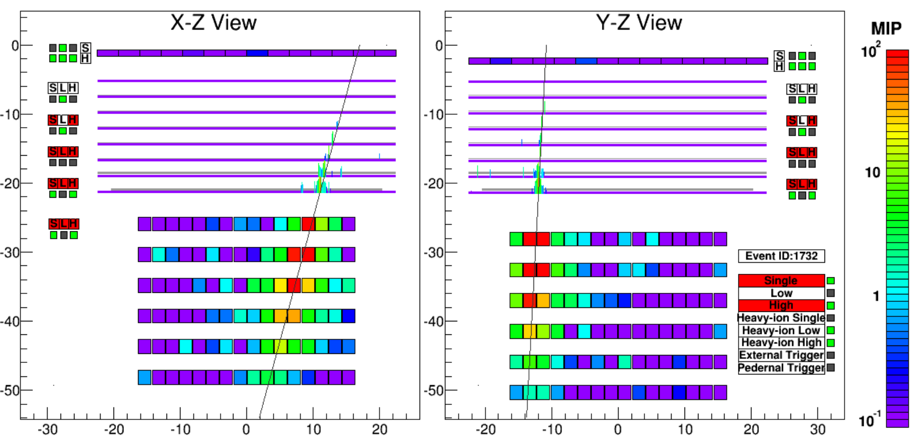

Unit in MIP

An Example of Highest Energy Events: Quick Look View

Energy deposit measurements in 4 different energy ranges

APD-H

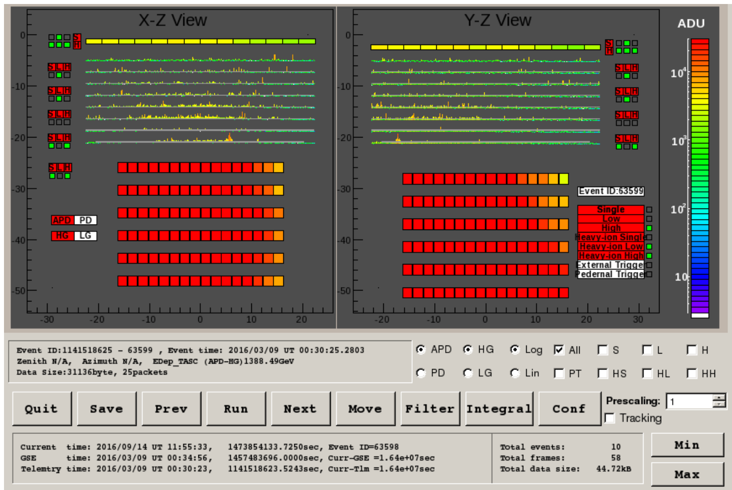

PD-H

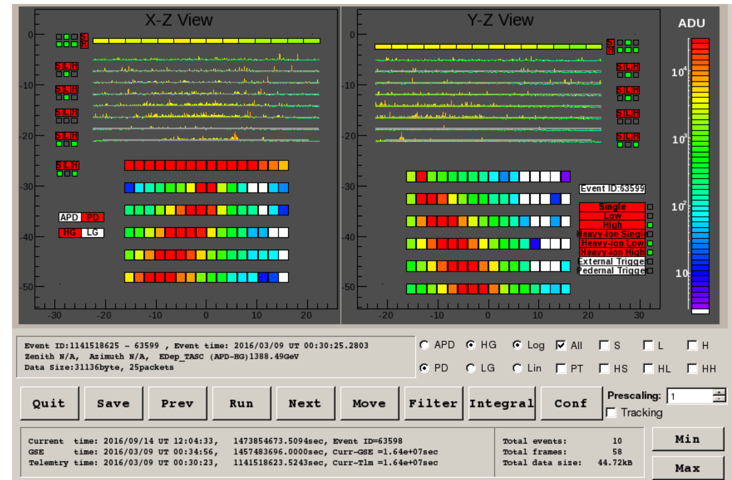

APD-L

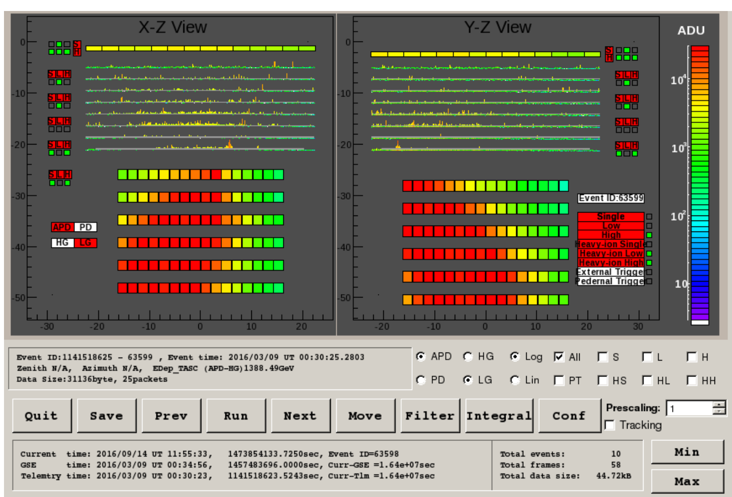

PD-L

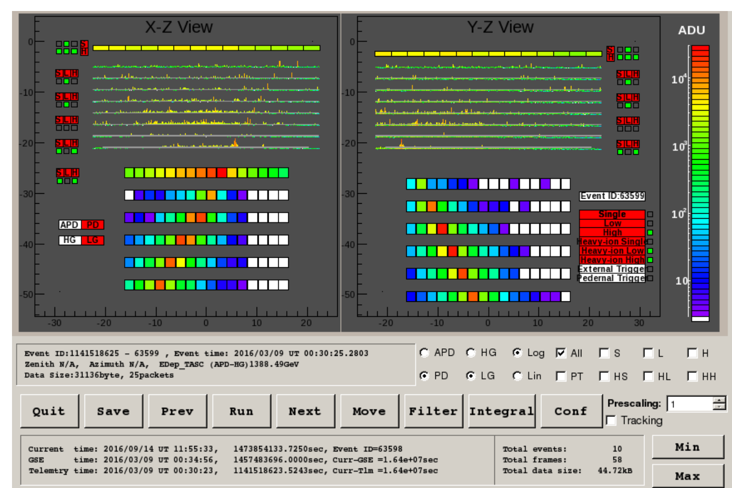

Preliminary Nuclei Measurements for Z=1-8

CHD charge resolution (2 layers combined) vs. Z

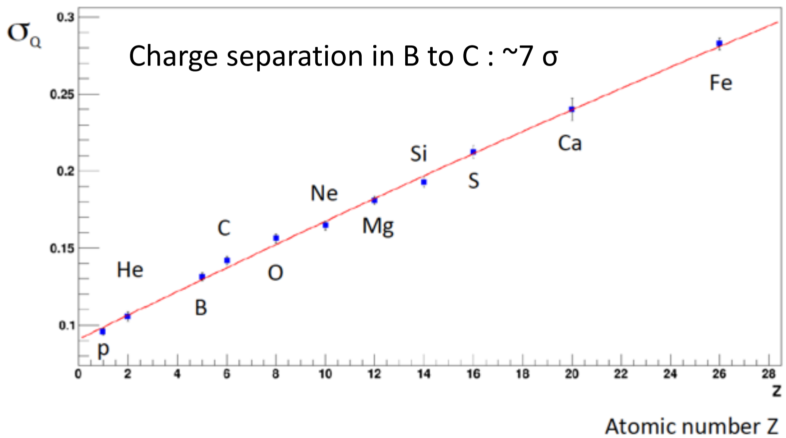

Charge resolution using multiple dE/dx measurements from the IMC scintillating fibers.

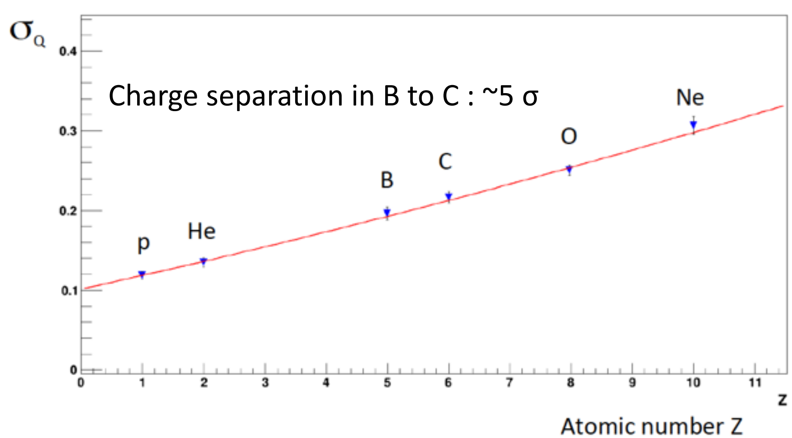

Non-linear response to Z^2 is corrected both in CHD and IMC using a model.

Charge resolution combined CHD+IMC

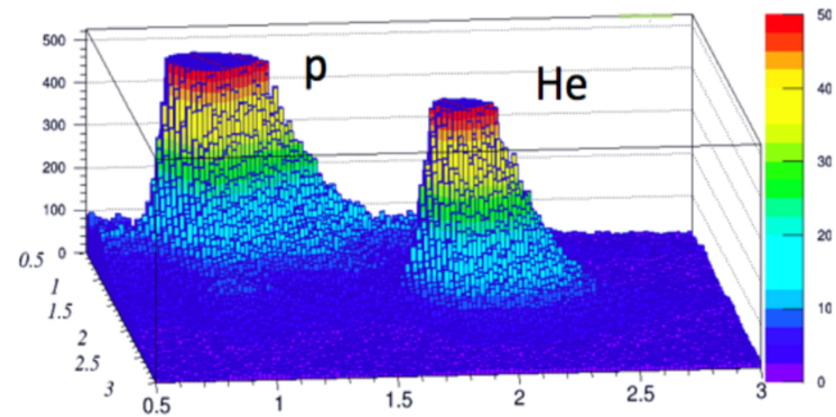

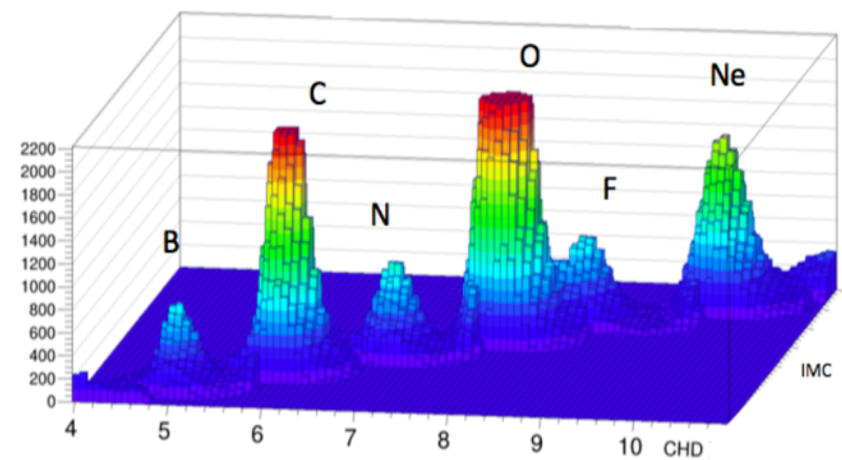

*) Plots are truncated to clearly present the separation.

A clear separation between p, He, ~ Z=8, can be seen from CHD+IMC data analysis.

Preliminary Proton Energy Spectrum

Preliminary proton flux $E^{2.7}$ from 50 GeV to 22 TeV

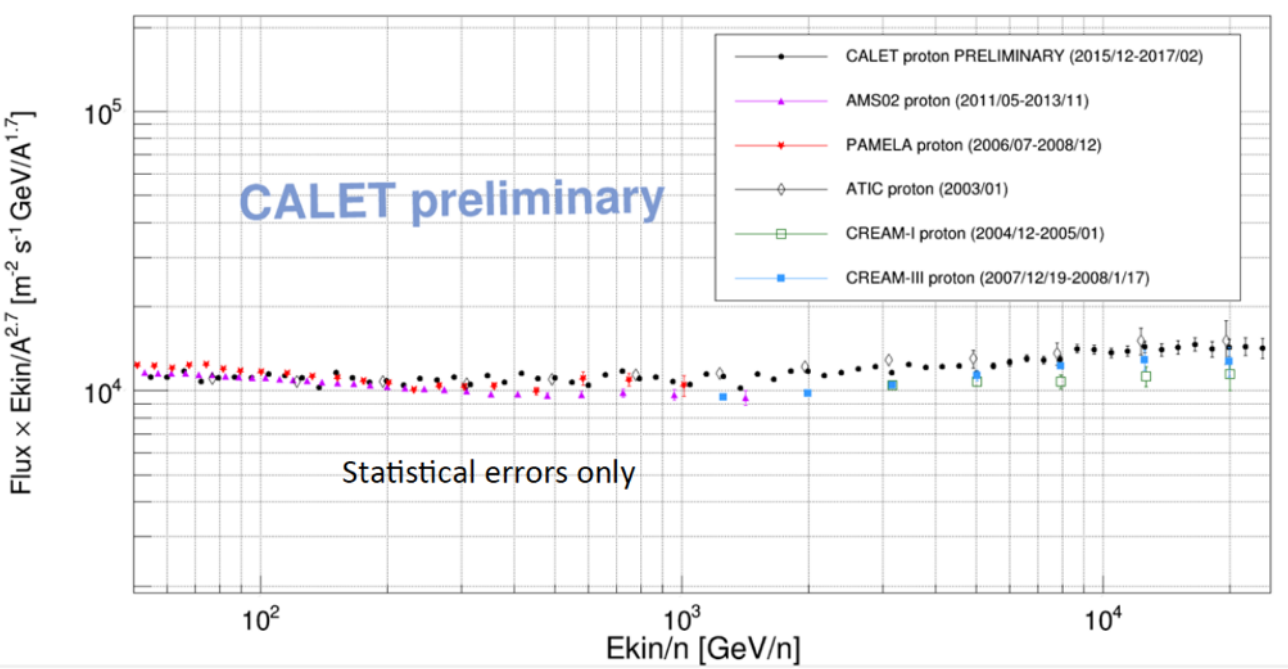

- 15 months of observation from December 1st , 2015 to February 28th, 2017
- subset of total acceptance: acceptance A (fiducial) with SΩ = 416 cm^2 sr
- Assessment of the systematic errors: IN PROGRESS

Data Analysis

- Proton Event Selection
  1) Fully-contained (Acceptance A) event in geometry
  2) Good tracking (KF)
  3) High Energy Trigger
  4) Charge selection Z=1
  5) Helium rejection cuts
  6) Electron rejection cuts
- Energy Unfolding by an ***energy overlap matrix*** from MC data

Preliminary Nuclei Measurements for Z= 8~26

Independent analysis is carried out for heavy nuclei in Z=8-26.

- Charge identification using correlation of CHD-X and CHD-Y:
  - require the charge consistency in CHD and IMC
  - efficiency of the consistency cuts is 65-70% for heavy nuclei (Z > 8)
- Quite similar charge resolutions were obtained by the different two analysis methods.

Charge correlation in CHD

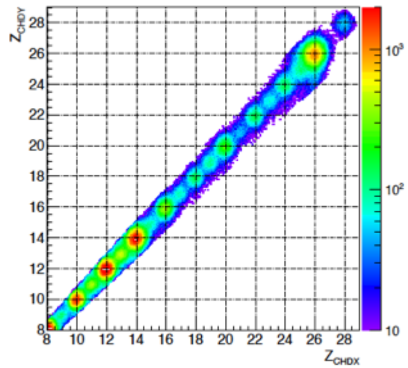

Charge distribution with CHD

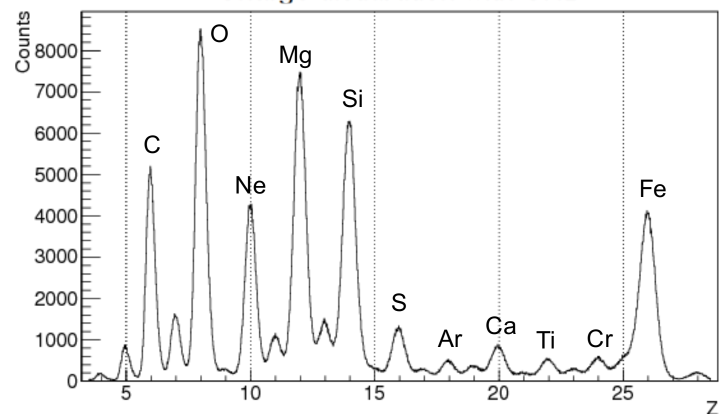

Flux measurement:

$$\Phi(E) = \frac{N(E)}{S\Omega\varepsilon(E)T\Delta E}$$

$N(E)$	Events in unfolded energy bin
$S\Omega$	Geometrical acceptance (A+B: 570 cm^2sr)
T	Live time (39 million seconds) (Oct.13 2015 – Mar.31 2017)
$\varepsilon(E)$	Efficiency of trigger and track reconstruction (>96%)
ΔE	Bin width

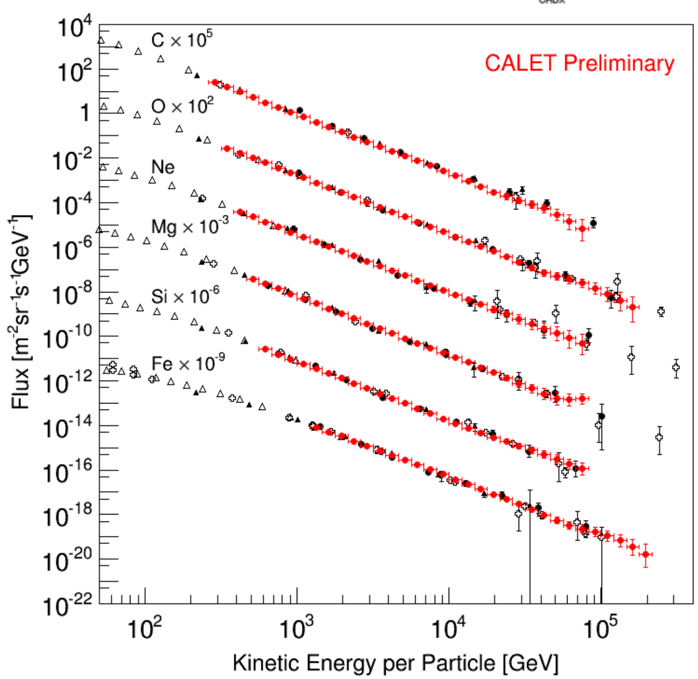

Data Analysis Method
(except similar way with light nuclei)

- Unfolding procedure based on ***Bayes' theorem*** is applied with response function from MC data.
- Charge selection efficiencies and contaminations from neighboring charged nuclei are also taken into account in the unfolding procedure.

Preliminary Ultra Heavy Nuclei Measurements for 26 < Z ≤ 40

- CALET measures the relative abundances of ultra heavy nuclei through $_{40}$Zr
- Trigger for ultra heavy nuclei:
  - signals of only CHD, IMC1+2 and IMC3+4 are required
  - ➡ an expanded geometrical acceptance (4000 cm^{2}sr)
- Energy threshold depends on the geomagnetic cutoff rigidity

Onboard trigger for UH events

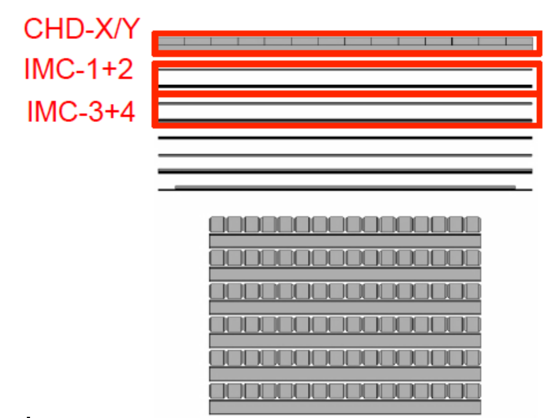

Data analysis

- ☐ Event Selection: Vertical cutoff rigidity > 4GV & Zenith Angle < 60 degrees
- ☐ Contamination from neighboring charge are determined by multiple-Gaussian function

Charge distribution

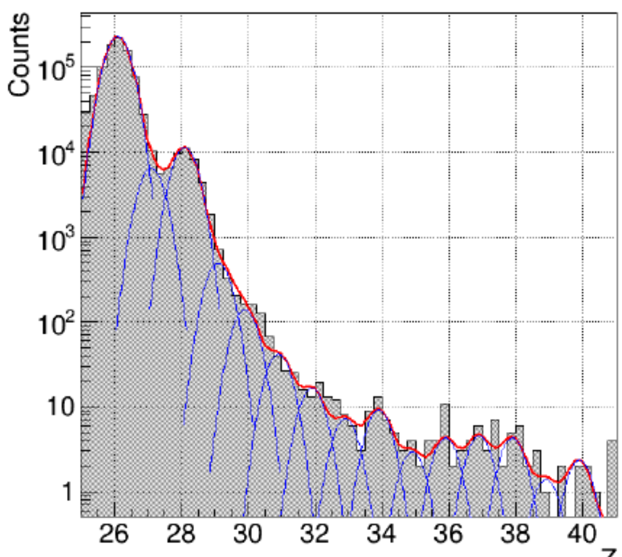

Relative abundance (Fe=1)

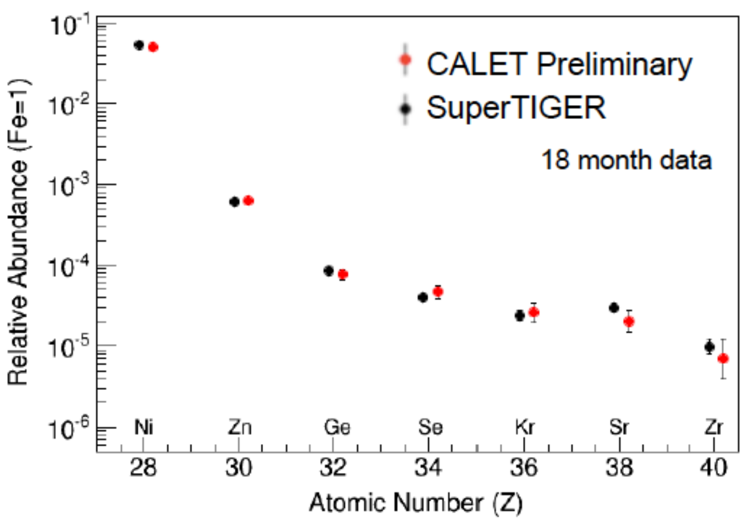

Electron Analysis: Characteristics of TeV Electron and Proton Showers

Physical Review Letters 119 (2017) 181101, 3 November 2017

Simple and high-efficiency electron identification is possible even at TeV.

⇒ CALET is best suited for observation of possible fine structures in the total electron spectrum in the trans-TeV region.

Flight Data (detector size in cm)

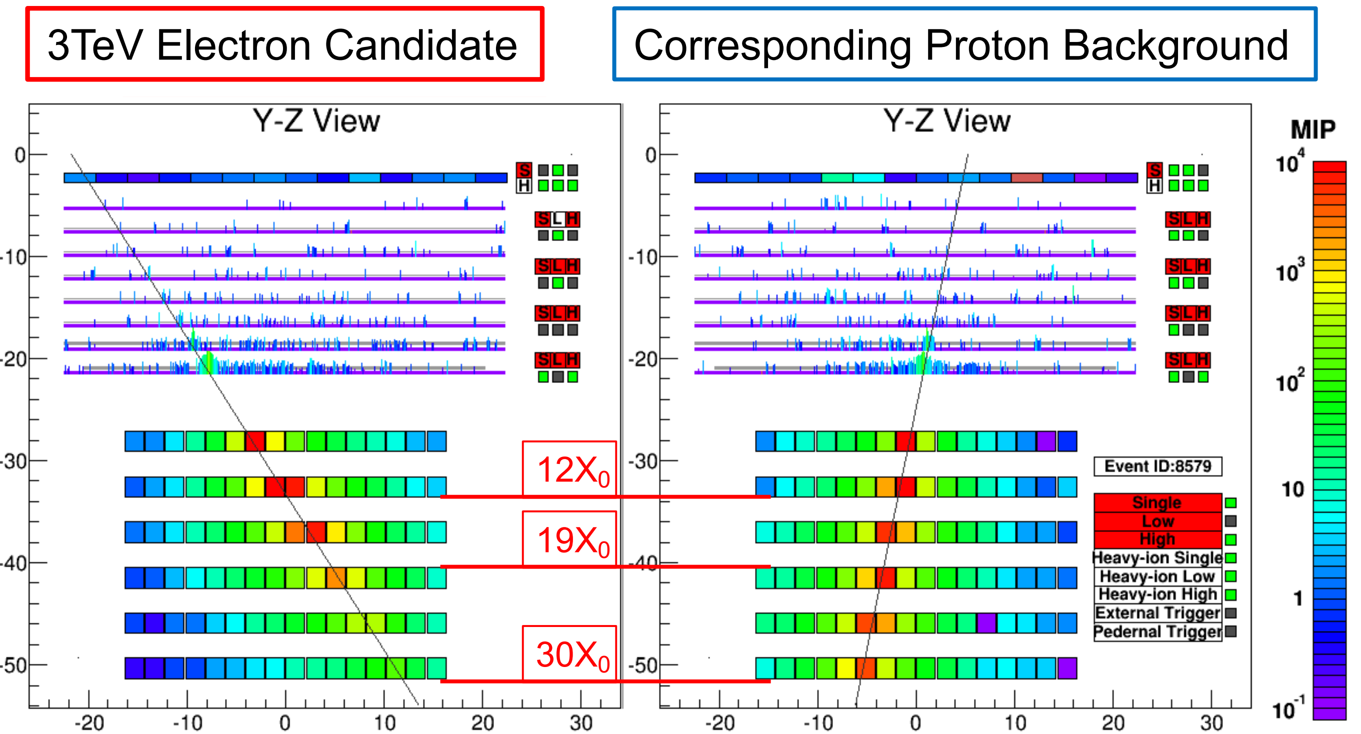

Electron / Proton Separation

Simple Two Parameter Cut

F_E: Energy fraction of the bottom layer sum to the whole energy deposit sum in TASC

R_E: Lateral spread of energy deposit in TASC-X1

Cut Parameter K is defined as follows:

$$K = \log_{10}(F_E) + 0.5\, R_E\ (/cm)$$

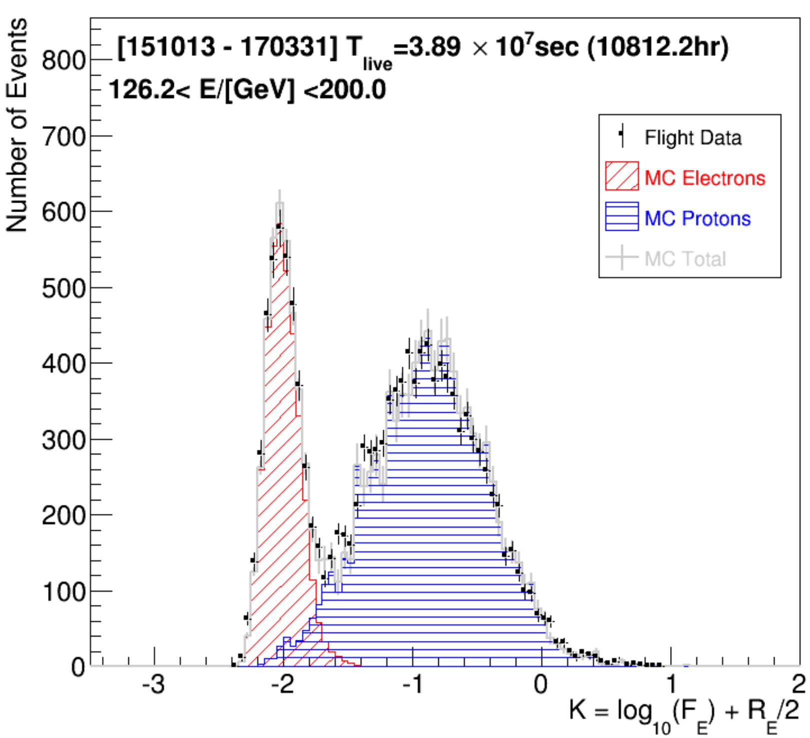

Boosted Decision Trees (BDT)

In addition to the two parameters in the left, TASC and IMC shower profile fits are used as discriminating variables.

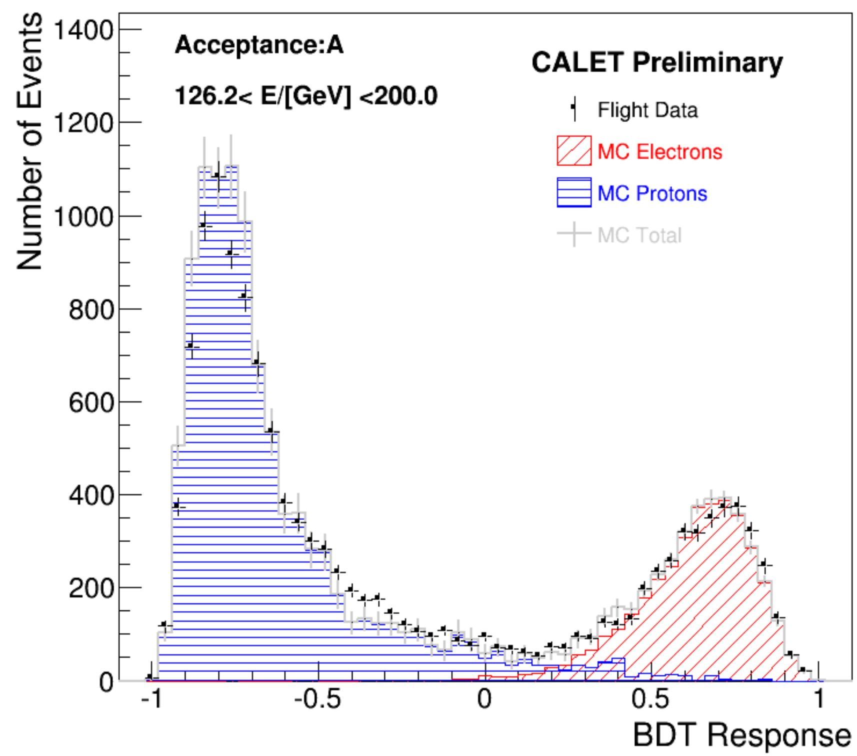

e/p Discrimination Power by the Analysis of BDT and K parameter

Distribution of BDT Response

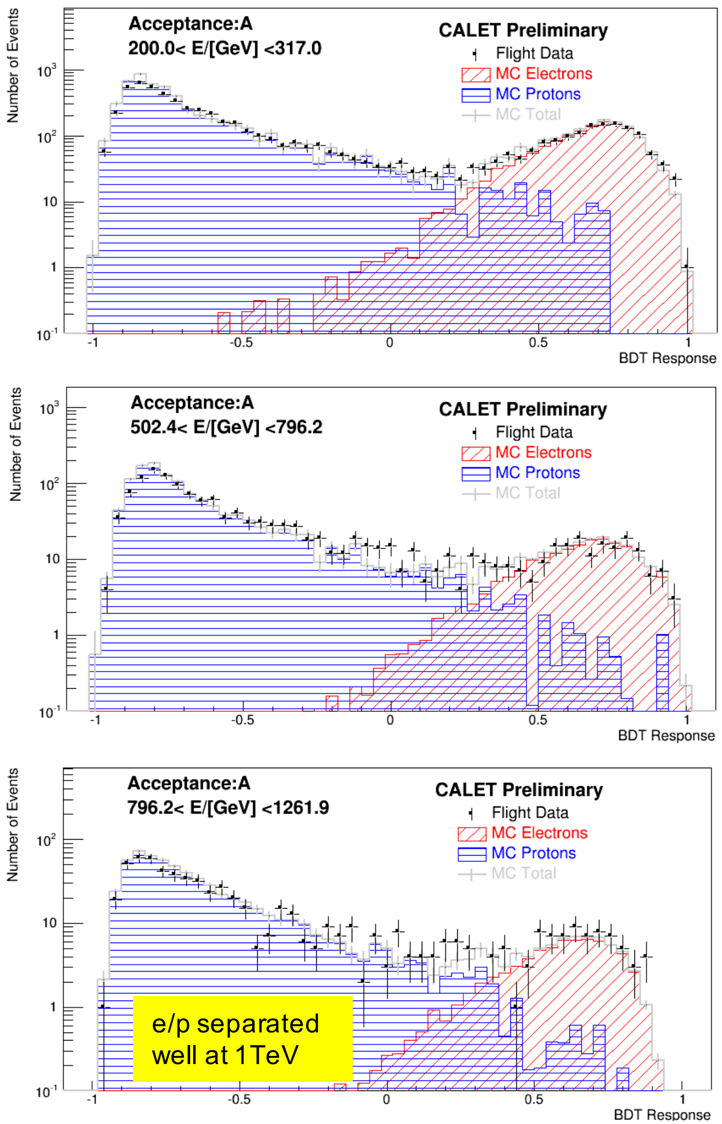

Electron Efficiency

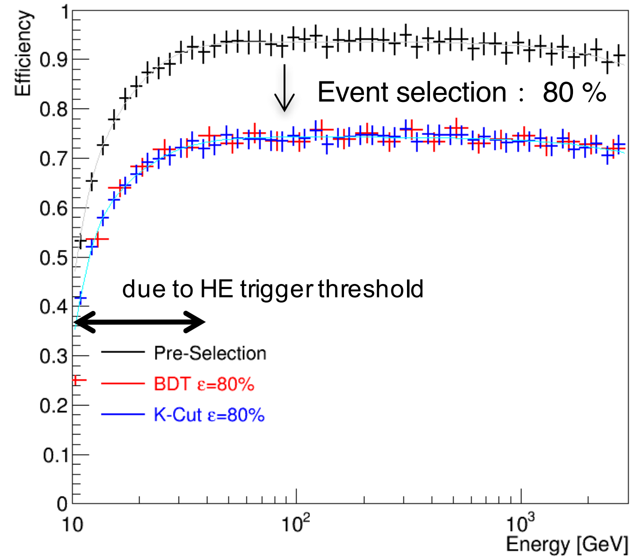

Proton contamination Ratio

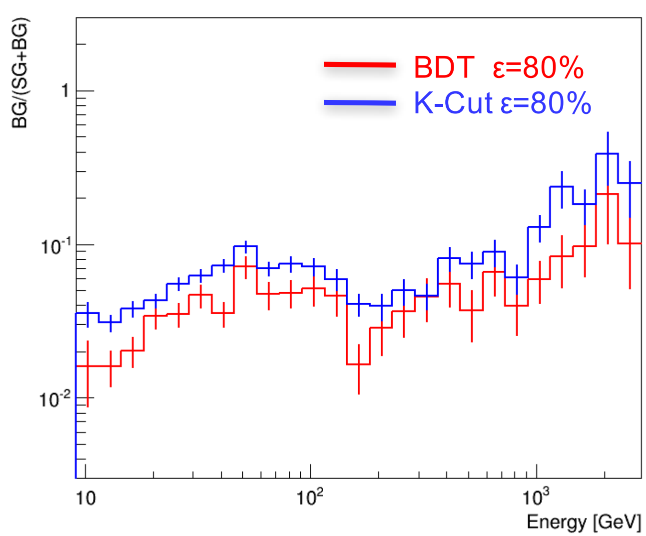

- Constant and high efficiency is the key point in our analysis.
- The efficiencies both of K-cut and BDT have very similar dependence on energies.
- Resultant electron efficiency after pre-selection and e/p separation is considerably high (~70%) and very constant over HE trigger threshold.
- Simple two parameter cut is used in the lower energy region (< 500GeV) , while the difference in resultant spectrum are taken into account in the systematic uncertainty.
- The proton contamination in 10 GeV-1 TeV is 2 - 5 %, and 5-10 % over 1 TeV using BDT analysis.
- (much better in near future by improvement of analysis)

Systematic Uncertainties in Derivation of Energy Spectrum

Stability of resultant flux are intensively studied in the large parameter space (i.e., viable choices to derive spectrum)

- Normalization:
  - Live time
  - Radiation environment
  - Long-term stability
  - Quality cuts
- Energy dependent:
  - Tracking
  - charge ID
  - electron ID (K-Cut vs BDT)
  - BDT stability
    (vs efficiency & training)
  - MC model
    (EPICS vs Geant4)

Systematic uncertainty in electron selection by BDT

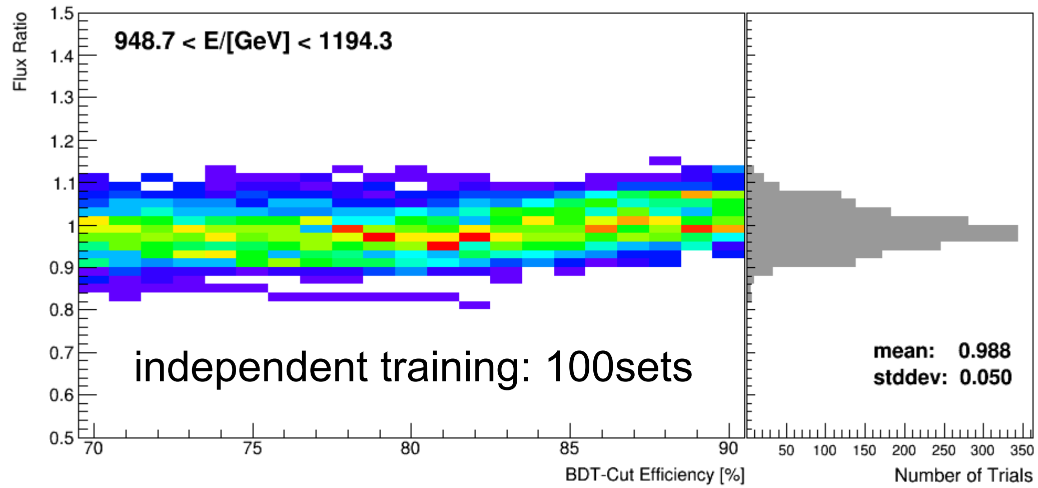

Total systematic uncertainty vs Energy

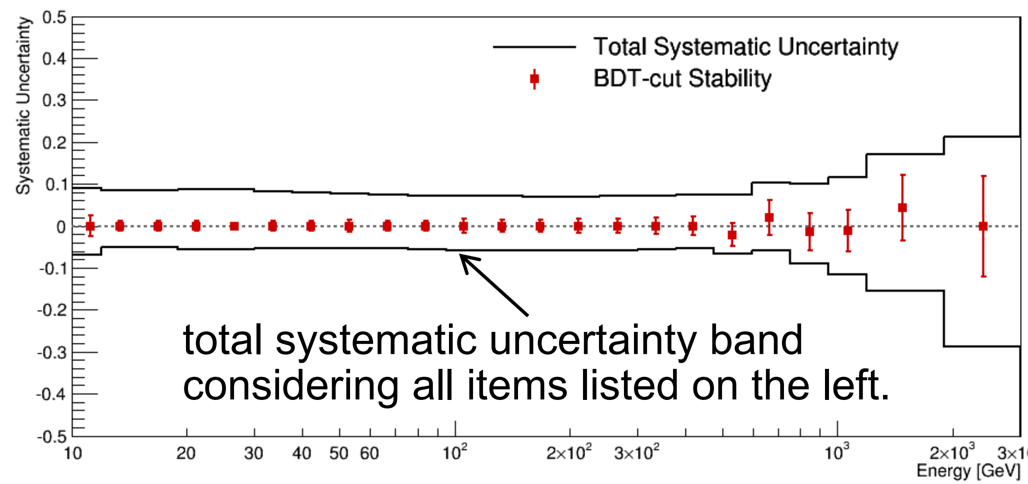

N.B. Energy scale uncertainty is not included in this analysis.

Calibration of Absolute Energy Scale Using Geomagnetic Rigidity Cutoff Energy

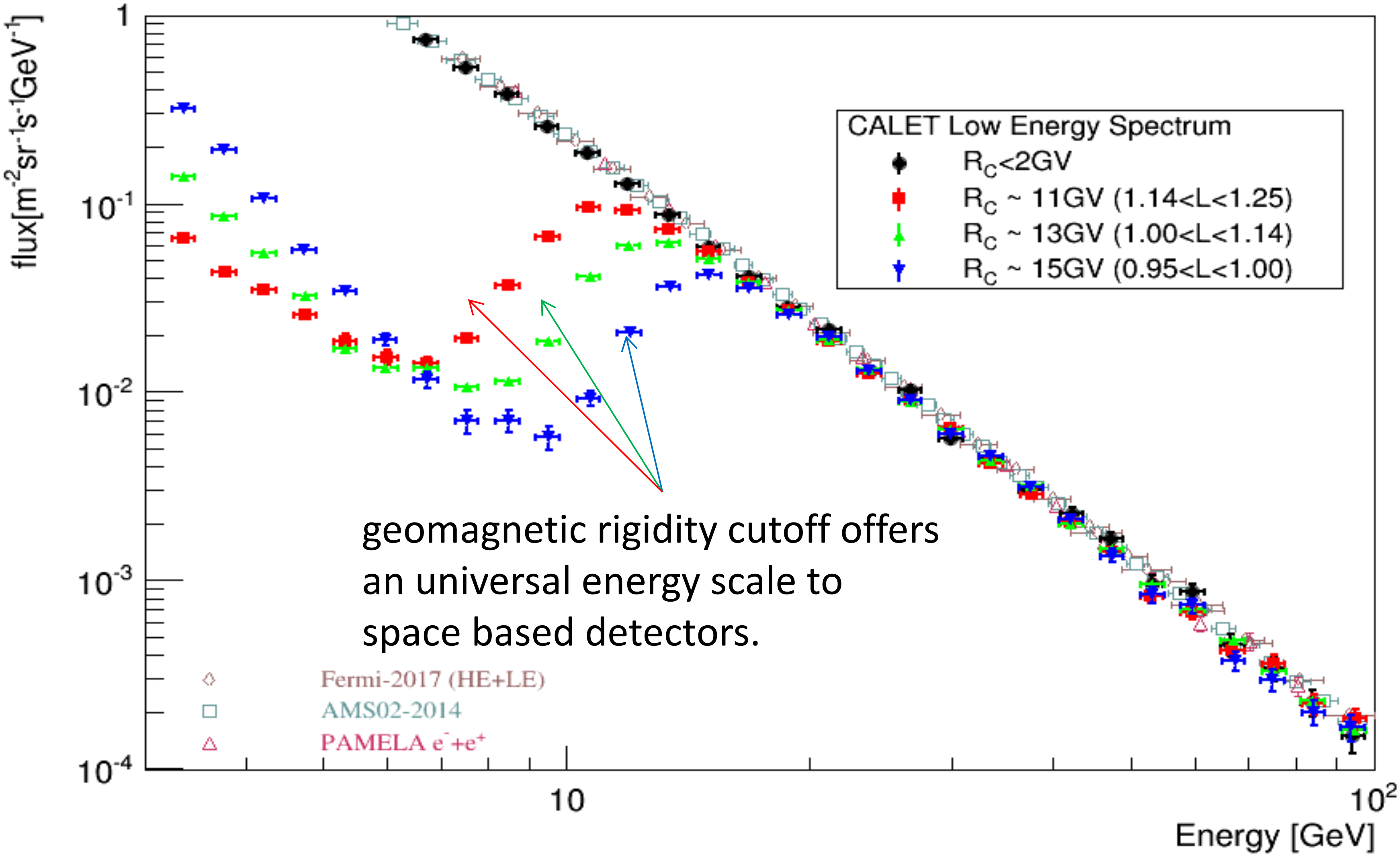

BEFORE CORRECTION

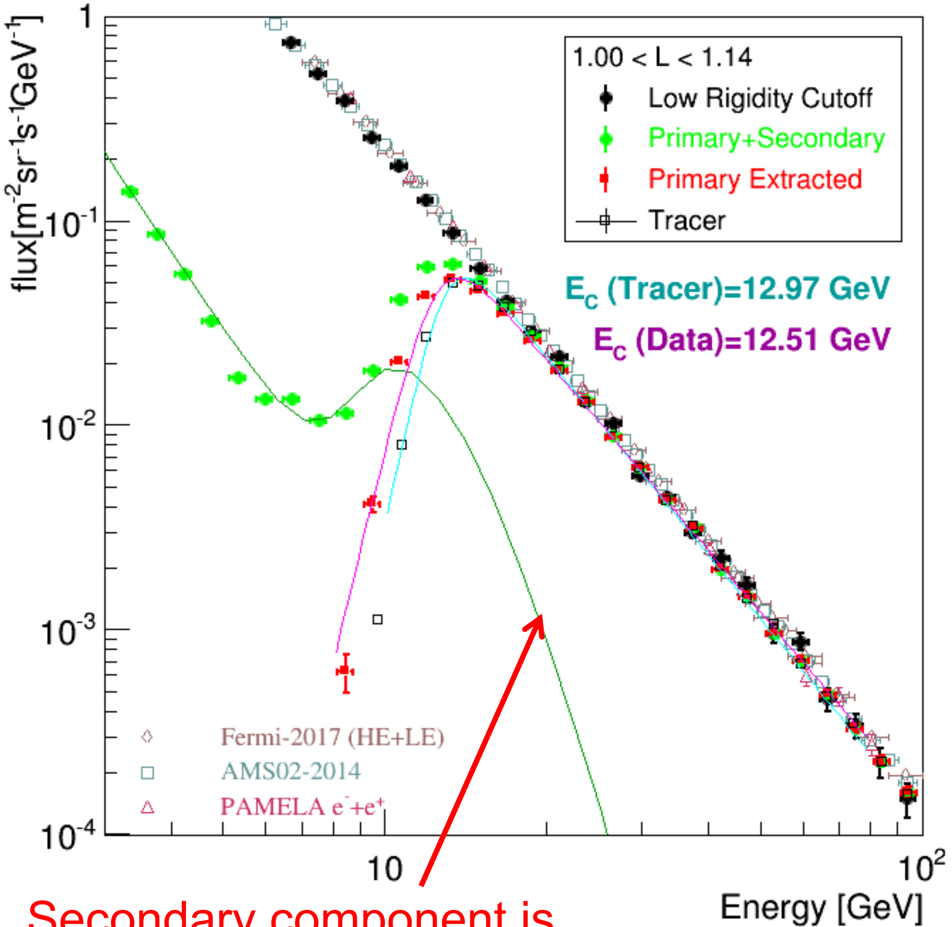

Secondary component is estimated using azimuthal distributions

- Performed in three different cutoff rigidity regions.
- Correction factor was found to be **1.035** compared to MIP calibration.

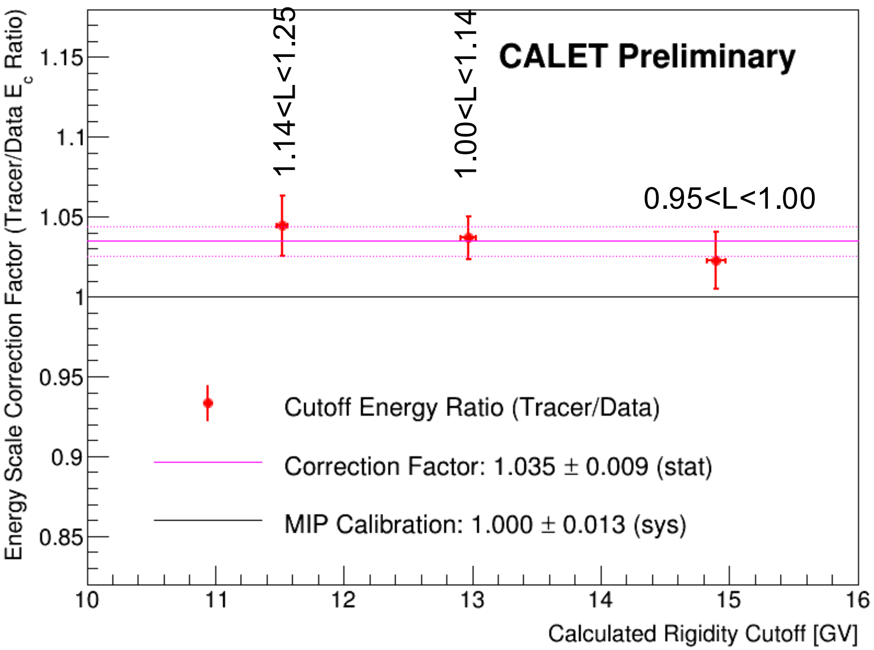

AFTER CORRECTION

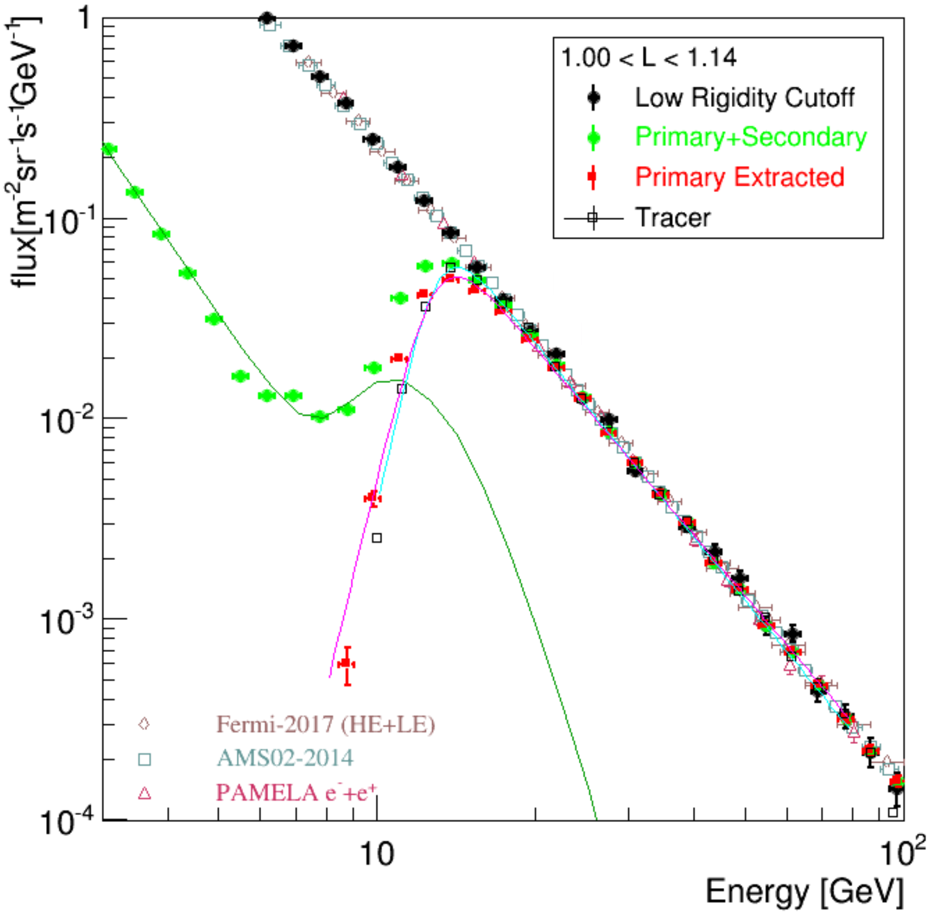

- Performed in three different cutoff rigidity regions.
- Correction factor was found to be **1.035** compared to MIP calibration.

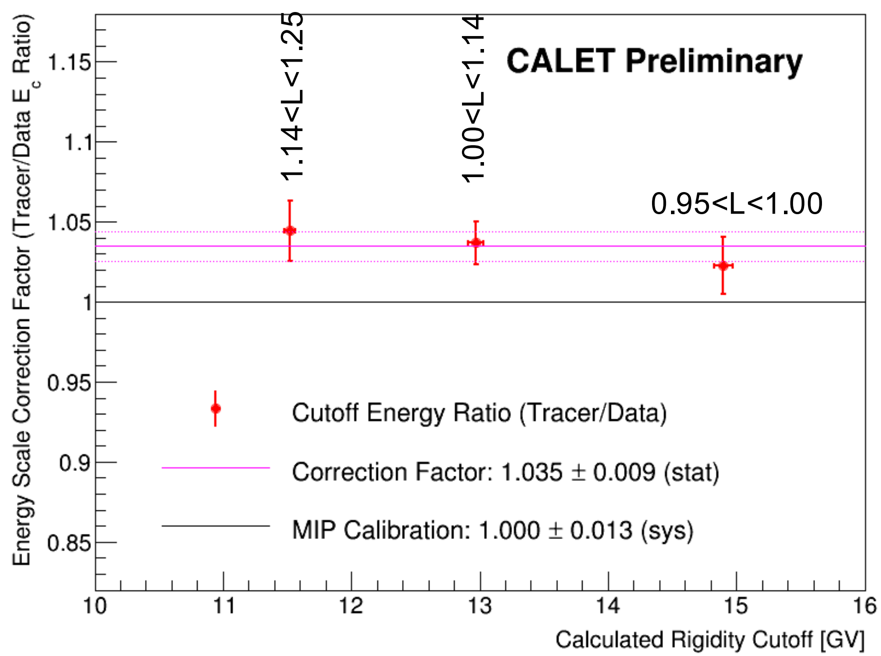

Since universal energy-scale calibration between different instruments is very important, we adopt the energy scale determined by rigidity cutoff to derive our spectrum.

Total (e^++e^-) Electron Energy Spectrum in 10 GeV～3TeV

- Geometry Condition: SΩ= 570.3 cm^{2}sr (Fully Contained: 55% for all acceptance)
- Live Time: 2015/10/13—2017/06/30 （x 0.85) => T= 4.57 x 10^7 sec
- Exposure: SΩT = 2.64 x 10^6 m^2 sr sec less than 20% of full analysis for 5 years

Physical Review Letters 119 (2017) 181101, 3 November 2017

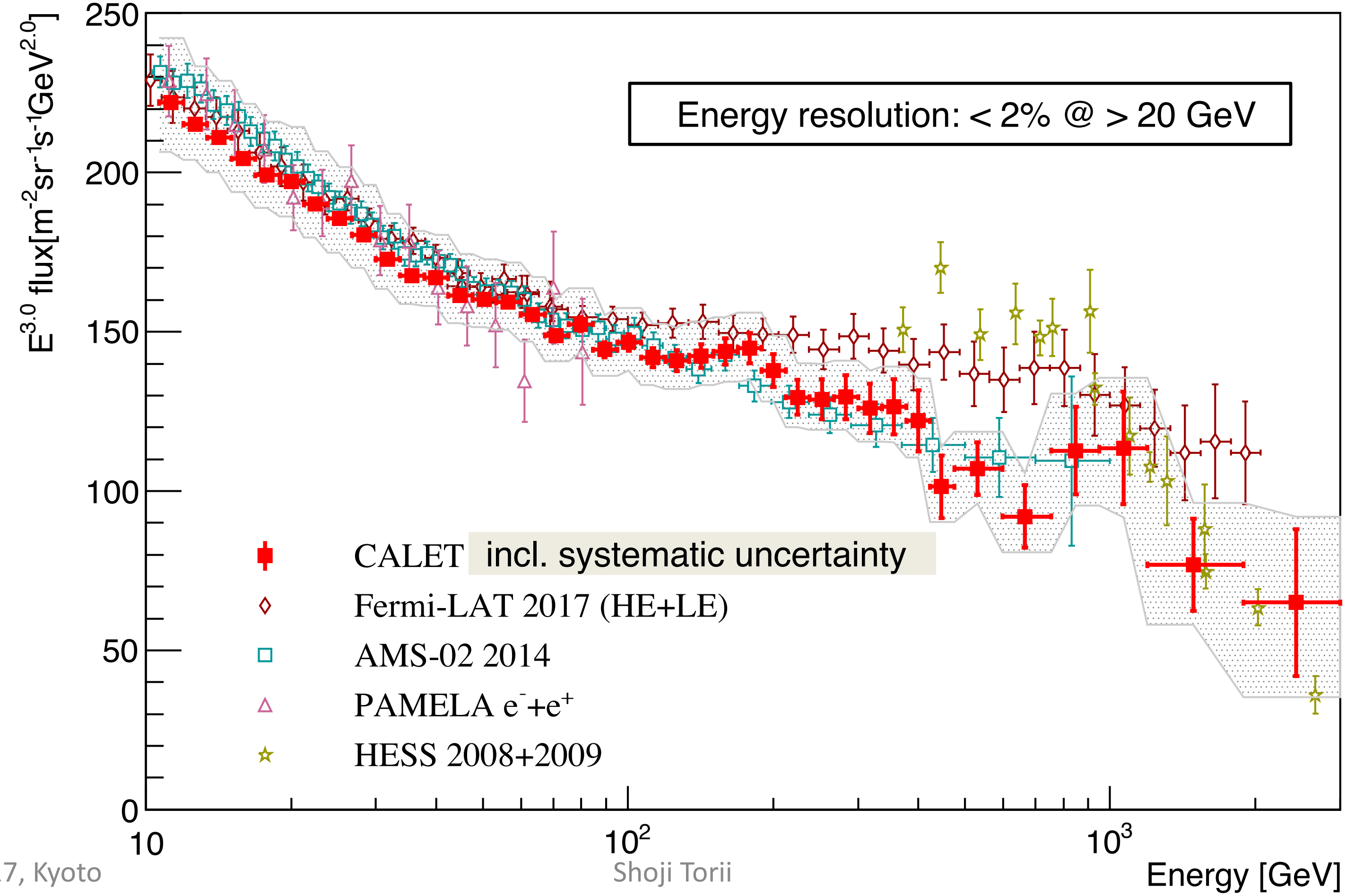

Interpretation of the CALET Results Related to the Positron Flux by AMS-02

- Additional source of cosmic ray positron and electron contributes equally to positrons and electrons [Kounine et al., ICRC 2017 Highlight Talk]
- The spectral feature of the additional component was studied with the combined fit:

$$\Phi_e^+ = \frac{E^2}{\tilde{E}^2}\left\{C_s\tilde{E}^{-\gamma_s} + C_c\tilde{E}^{-\gamma_c}\exp(-\tilde{E}/E_c)\right\} \quad \Phi_e^- = \frac{E^2}{\tilde{E}^2}\left\{C\tilde{E}^{-\gamma(\tilde{E})} + C_s\tilde{E}^{-\gamma_s} + C_c\tilde{E}^{-\gamma_c}\exp(-\tilde{E}/E_c)\right\} \quad \tilde{E} = E + \Psi$$

Positron Spectrum

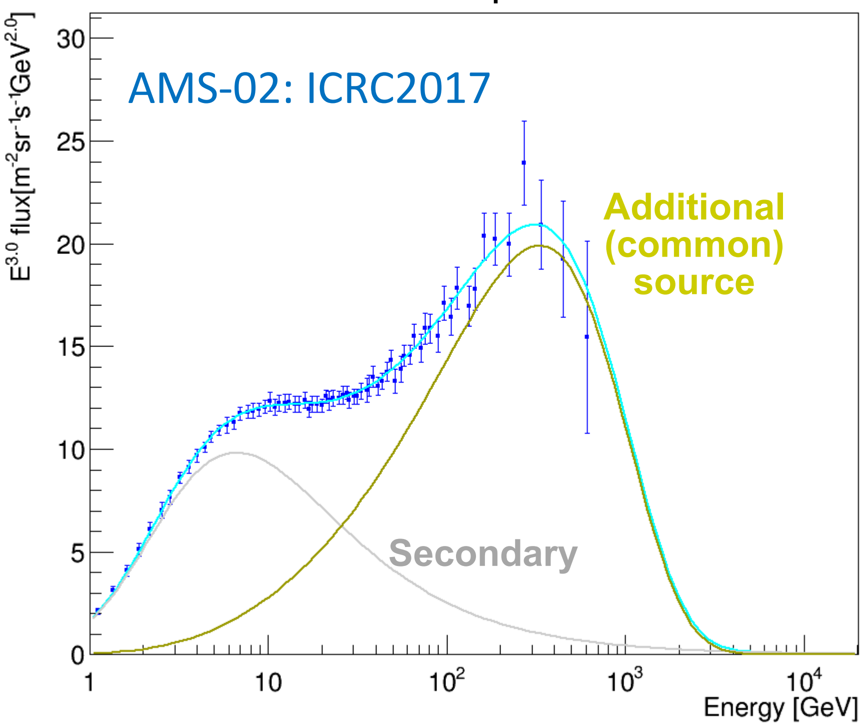

(Electron + Positron) Spectrum

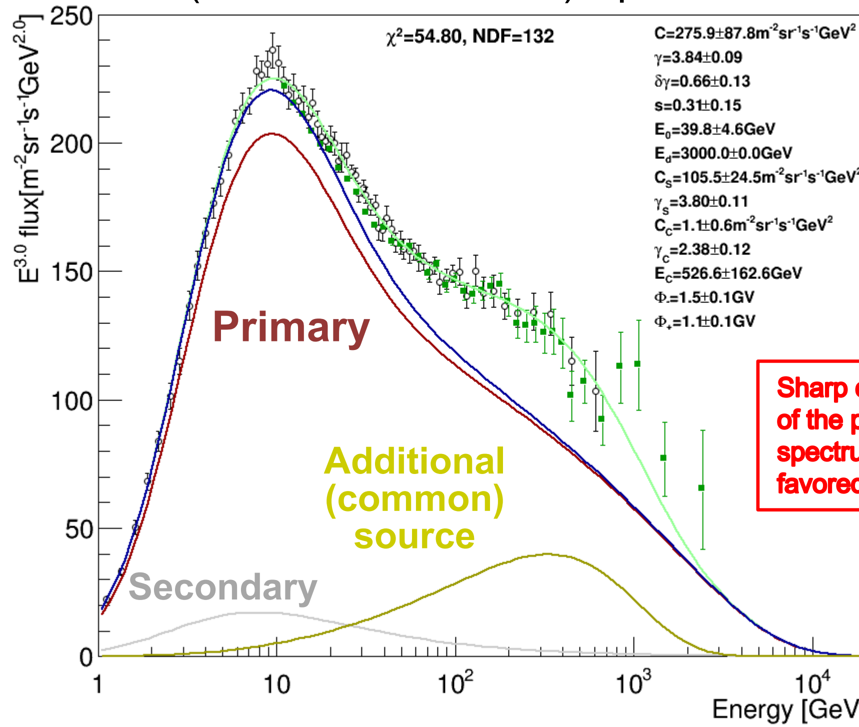

Sharp cutoff of the positron spectrum is favored.

Using precisely measured all-electron spectrum ($e^- + e^+$), it is possible to quantitatively probe the highest energy part of e^+ and e^- from the common source component.

Constraint on Contribution from the Local SNR

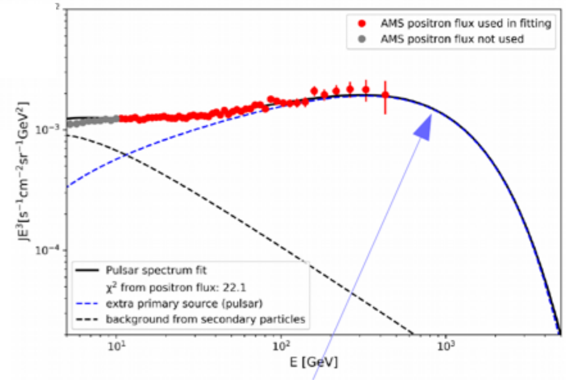

parameters for Vela calculation (case used in ICRC anisotropy study):

$$D_0 = 1.3\cdot 10^{28} cm^2/s \;\; ; \;\; \delta = 0.6 \left(R > 300\,GV \rightarrow 0.33 \right) \;\; ; \;\; L = \pm 3\,kpc$$

$$\gamma_i = 2.92 - \delta = 2.32 \quad E_{cut} = 100\,TeV$$

instantaneous release of CR from the SNR assumed

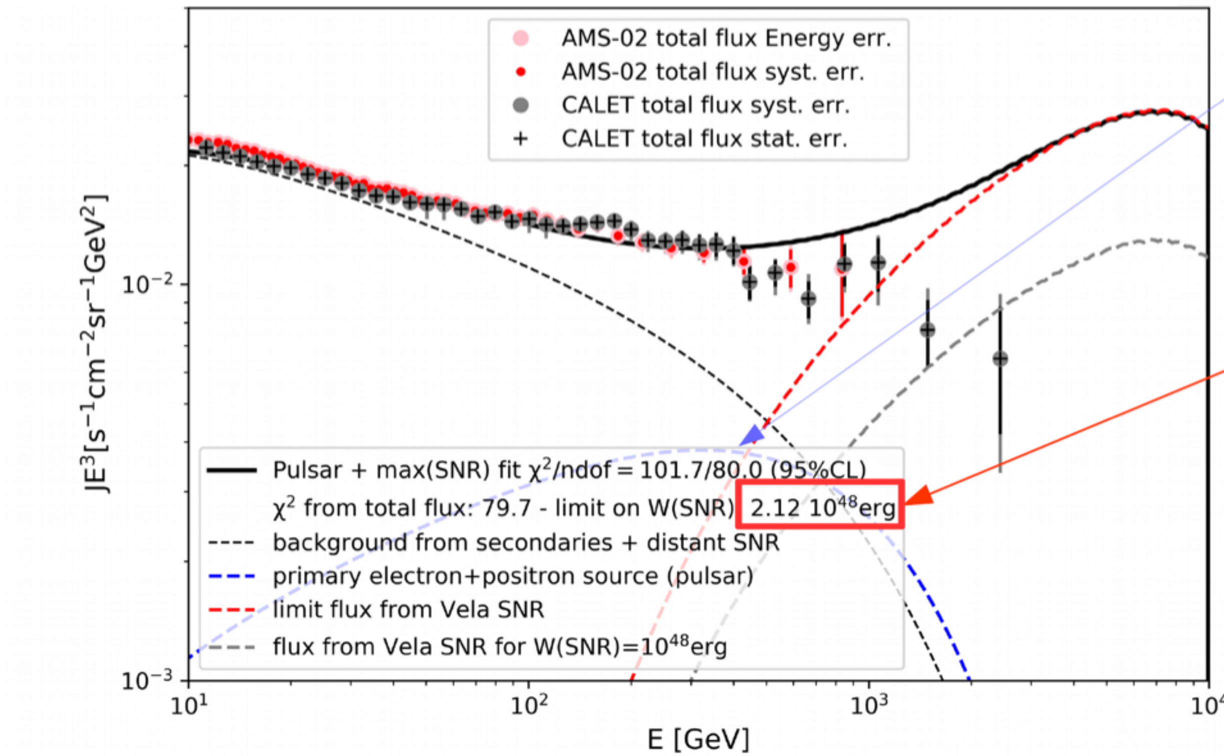

Extra primary source for positron excess → AMS-02 positron flux is also fitted

Limit on energy emitted by Vela

Even with the limited statistics and limited energy range, CALET data already start to constrain the contribution from the local SNR. The use of full CALET data will severely constrain or discover the local SNR.

Talk by H. Motz et al. on Dec.13

Limits on Dark Matter and Nearby Astrophysical Sources from the CALET Electron+Positron Spectrum

Comparison with DAMPE results

Nature Letters 552 (2017) 63, 7 December 2017

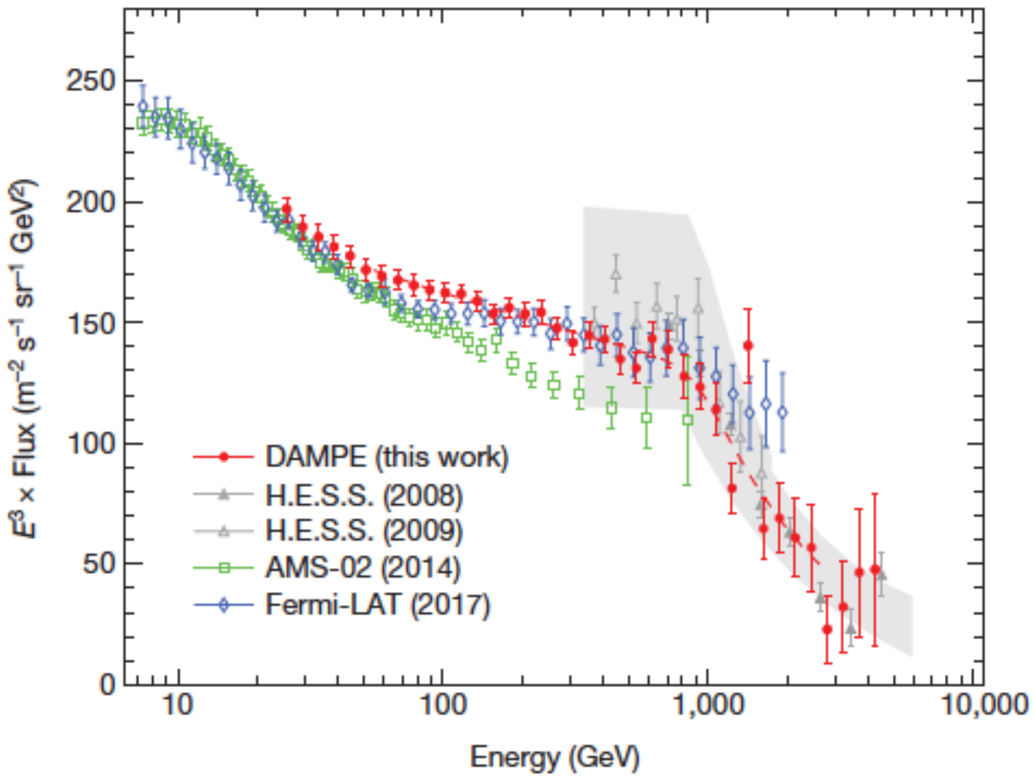

Figure 2 | The CRE spectrum (multiplied by E^3) measured by DAMPE. The red dashed line represents a smoothly broken power-law model that best fits the DAMPE data in the range 55 GeV to 2.63 TeV. Also shown are the direct measurements from the space-borne experiments AMS-02[14] and Fermi-LAT[16], and the indirect measurement by the H.E.S.S. Collaboration (the grey band represents its systematic errors apart from the approximately 15% energy scale uncertainty)[17,18]. The error bars ($\pm 1\sigma$) of DAMPE, AMS-02 and Fermi-LAT include both systematic and statistical uncertainties added in quadrature.

Comparison with DAMPE results

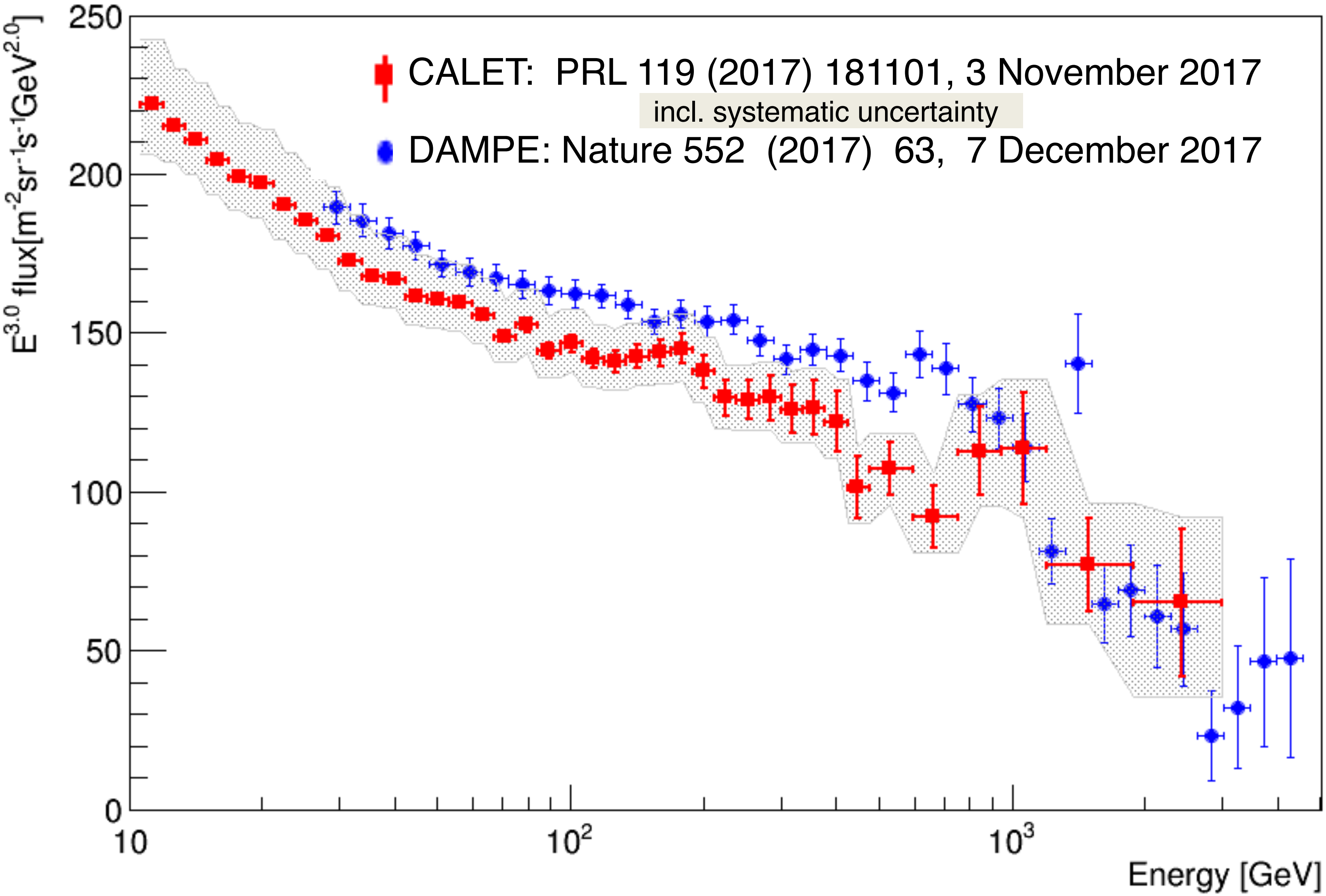

CALET γ–ray Sky in LE (>1GeV) Trigger

Exposure

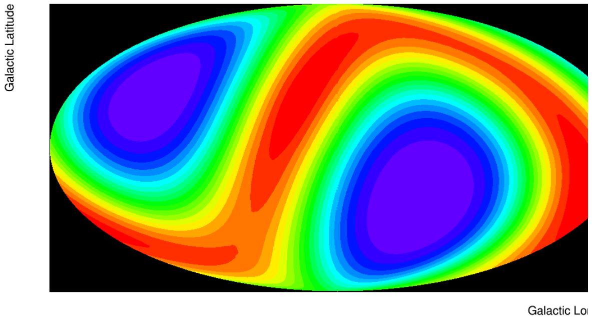

Exposure is limited to low latitude region
=> |declination| > 60 deg is hardly seen in LE gamma-ray trigger mode.

151013—170228 E>1GeV Galactic Coordinate

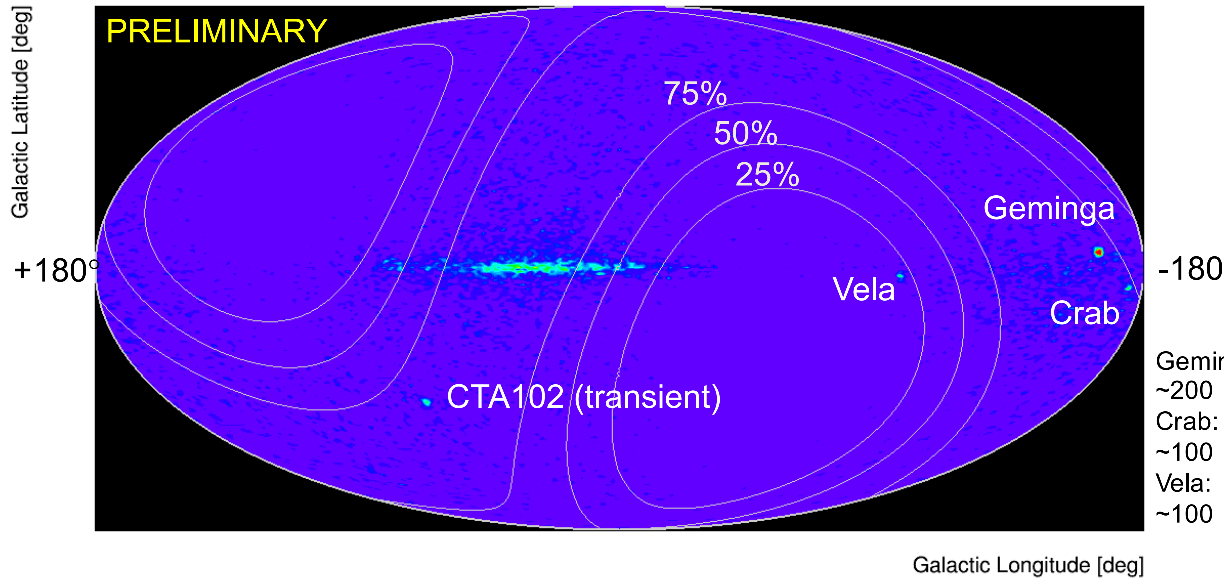

Geminga: ~200
Crab: ~100
Vela: ~100

Projection to Galactic Latitude

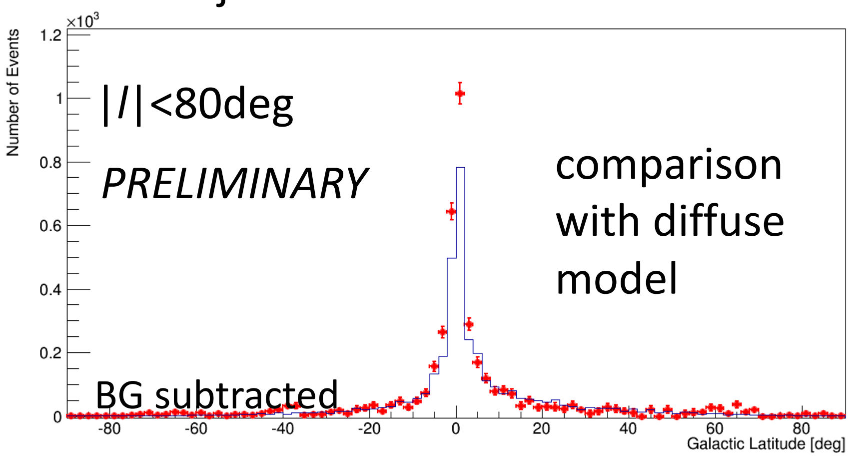

Galactic Diffuse Spectrum

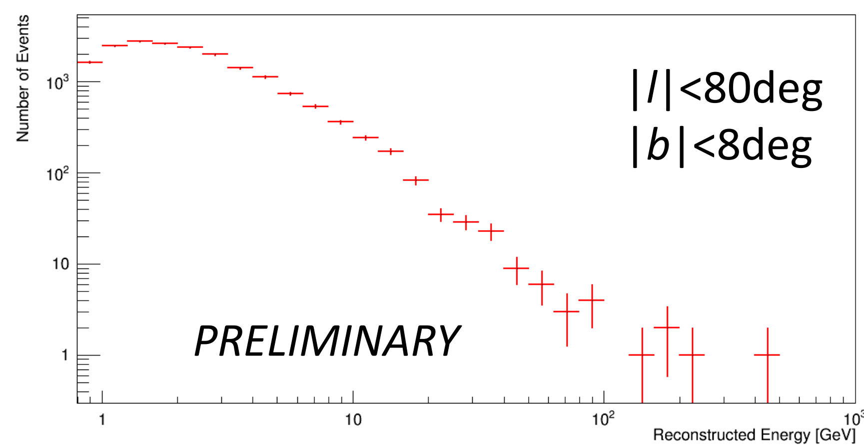

*) Contribution from point sources is not included in the model

Strong GeV Gamma-ray Activi from Blazar CTA 102

Reported to ATEL by AGILE, Fermi, DAMPE in GeV

⇒ Also detected by CALET

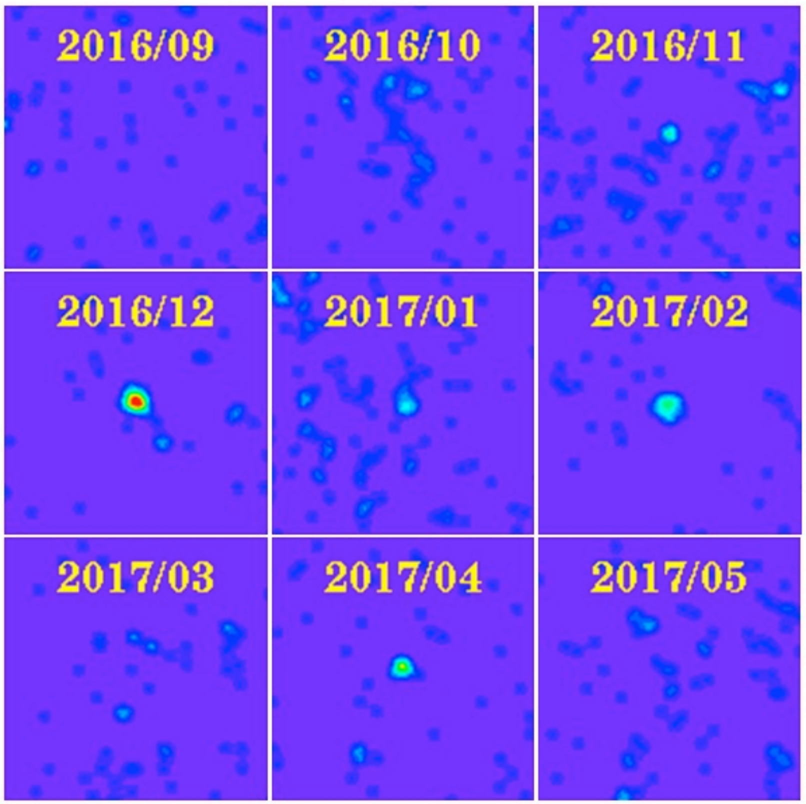

CALET observations of CTA 102 in the months 2015/10 through 2017/04.

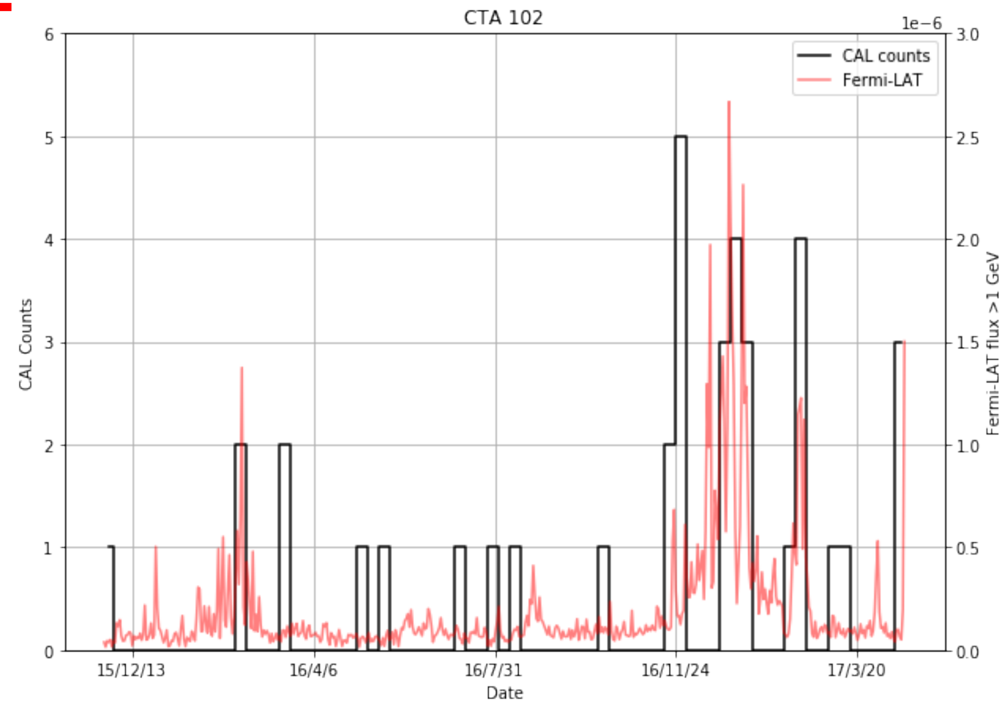

Comparing this to the Fermi-LAT flux above 1 GeV for the same time period, it is clear that the enhancements are correlated with flares that are also reported by the Fermi-LAT collaboration

CALET γ–ray Sky in HE (>10GeV) Trigger

Exposure

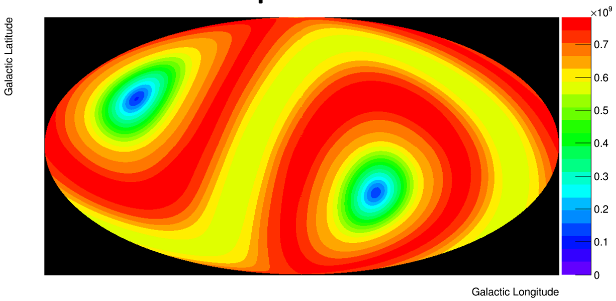

HE trigger is always ON
=> Exposure determined by the ISS orbit and FOV is more uniform than LE trigger.

151013—170228 E>10GeV Galactic Coordinate

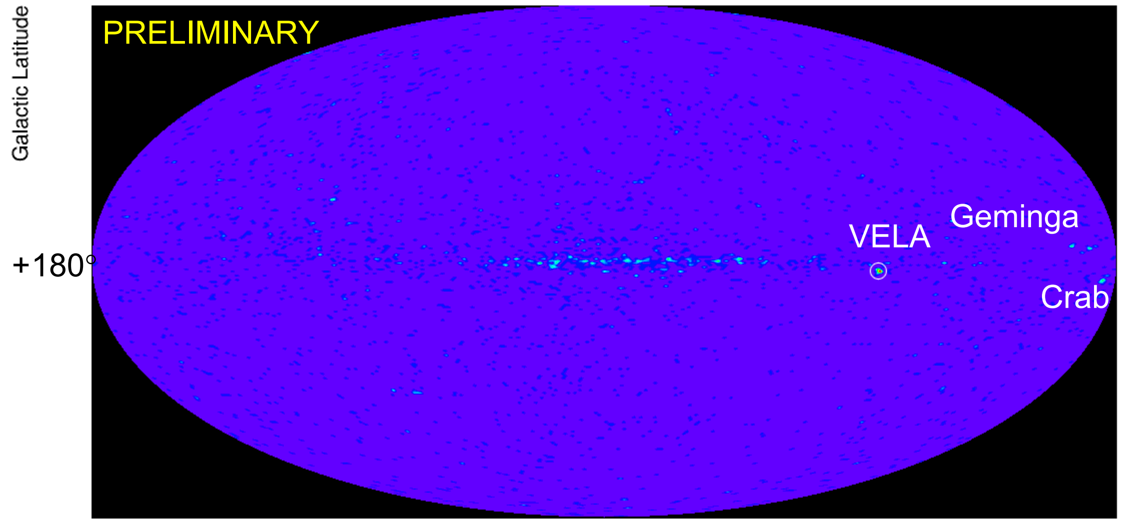

Geminga: ~10
Crab: ~20
Vela: ~20

Vela, Crab and Geminga are identified.

Projection to Galactic Latitude

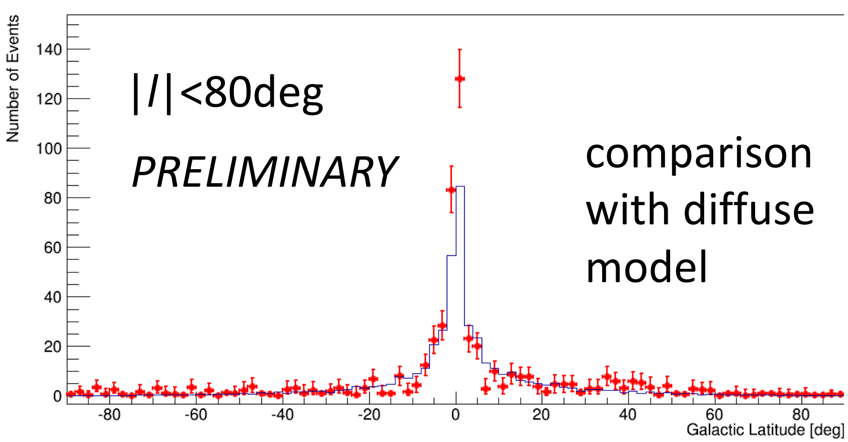

Diffuse Spectrum

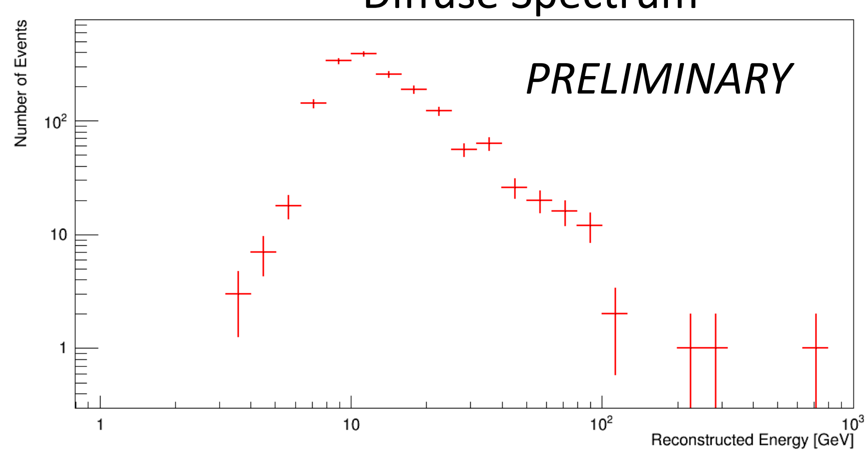

contribution from point sources is not included in the model

CALET UPPER LIMITS ON X-RAY AND GAMMA-RAY COUNTERPARTS OF GW 151226

Astrophysical Journal Letters 829:L20(5pp), 2016 September 20

The CGBM covered 32.5% and 49.1% of the GW 151226 sky localization probability in the 7 keV - 1 MeV and 40 keV - 20 MeV bands respectively. We place a 90% upper limit of 2×10^{-7} erg cm^{-2} s^{-1} in the 1 - 100 GeV band where CAL reaches 15% of the integrated LIGO probability (~1.1 sr). The CGBM 7 σ upper limits are 1.0×10^{-6} erg cm^{-2} s^{-1} (7-500 keV) and 1.8×10^{-6} erg cm^{-2} s^{-1} (50-1000 keV) for one second exposure. Those upper limits correspond to the luminosity of 3-5 $\times 10^{49}$ erg s^{-1} which is significantly lower than typical short GRBs.

CGBM light curve at the moment of the GW151226 event

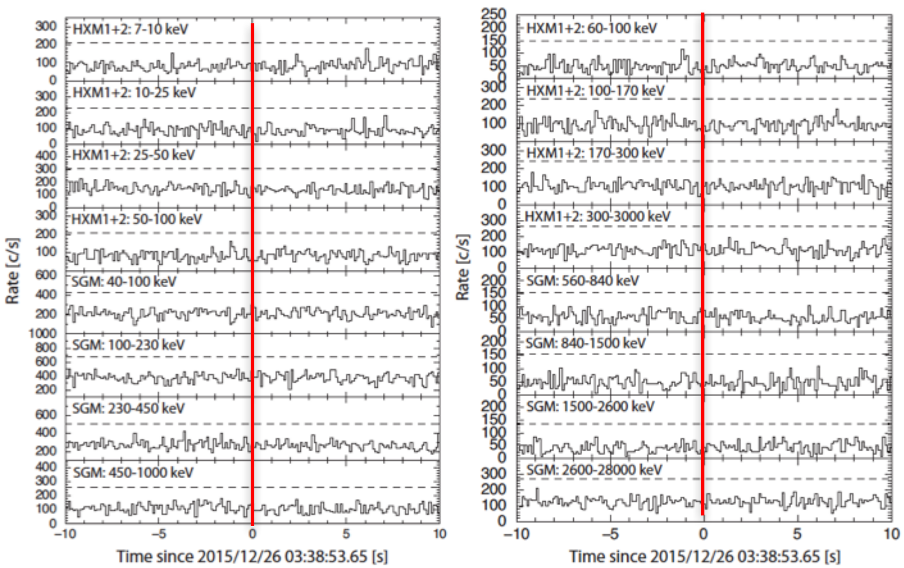

Figure 1. The CGBM light curves in 0.125 s time resolution for the high-gain data (left) and the low-gain data (right). The time is offset from the LIGO trigger time of GW 151226. The dashed-lines correspond to the 5 σ level from the mean count rate using the data of ±10 s.

Upper limit for gamma-ray burst monitors and Calorimeter

HXM: 7-500 keV

SGM: 50-1000 keV

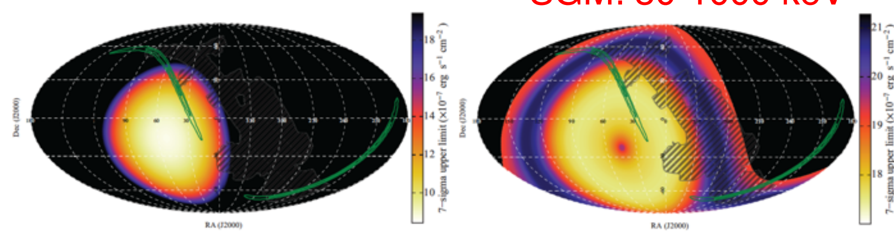

Figure 2. The sky maps of the 7 σ upper limit for HXM (left) and SGM (right). The assumed spectrum for estimating the upper limit is a typical BATSE S-GRBs (see text for details). The energy bands are 7-500 keV for HXM and 50-1000 keV for SGM. The GW 151226 probability map is shown in green contours. The shadow of ISS is shown in black hatches.

Calorimeter: 1-100 GeV

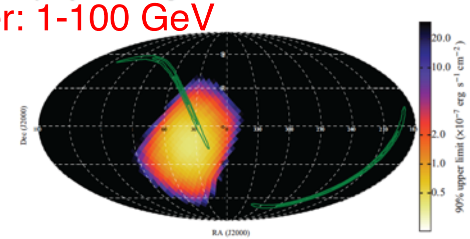

Figure 3. The sky map of the 90% upper limit for CAL in the 1-100 GeV band. A power-law model with a photon index of −2 is used to calculate the upper limit. The GW 151226 probability map is shown in green contours.

CALET's first publication NOT for Cosmic Rays

Accepted article online 25 APR 2016

Geophysical Research Letters

Relativistic electron precipitation at International Space Station: Space weather monitoring by Calorimetric Electron Telescope

Ryuho Kataoka[1,2], Yoichi Asaoka[3], Shoji Torii[3,4], Toshio Terasawa[5], Shunsuke Ozawa[4], Tadahisa Tamura[6], Yuki Shimizu[6], Yosui Akaike[4], and Masaki Mori[7]

[1]Space and Upper Atmospheric Sciences Group, National Institute of Polar Research, Tachikawa, Japan, [2]Department of Polar Science, School of Multidisciplinary Sciences, SOKENDAI (Graduate University for Advanced Studies), Tachikawa, Japan, [3]Research Institute for Science and Engineering, Waseda University, Shinjuku, Japan, [4]Department of Physics, Waseda University, Shinjuku, Japan, [5]Institute for Cosmic Ray Research, University of Tokyo, Kashiwa, Japan, [6]Institute of Physics, Kanagawa University, Yokohama, Japan, [7]Department of Physical Sciences, Ritsumeikan University, Kusatsu, Japan

Abstract The charge detector (CHD) of the Calorimetric Electron Telescope (CALET) on board the International Space Station (ISS) has a huge geometric factor for detecting MeV electrons and is sensitive to relativistic electron precipitation (REP) events. During the first 4 months, CALET CHD observed REP events mainly at the dusk to midnight sector near the plasmapause, where the trapped radiation belt electrons can be efficiently scattered by electromagnetic ion cyclotron (EMIC) waves. Here we show that interesting 5–20 s periodicity regularly exists during the REP events at ISS, which is useful to diagnose the wave-particle interactions associated with the nonlinear wave growth of EMIC-triggered emissions.

Space Weather is now a new topic of the CALET science !!

Relativistic Electron Precipitation

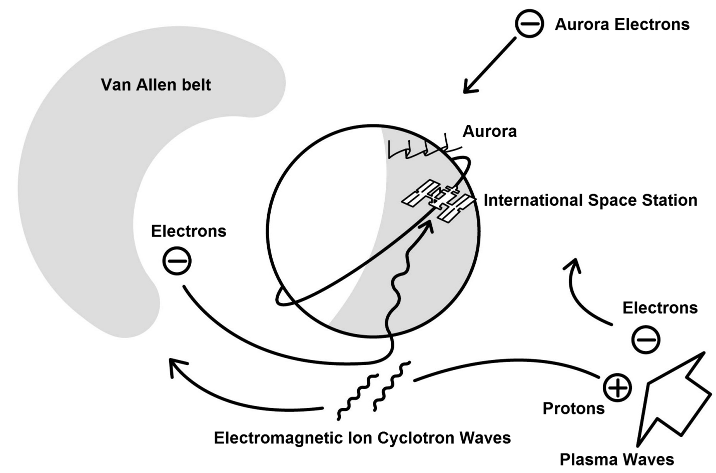

CHD X and Y count rate increase by REP

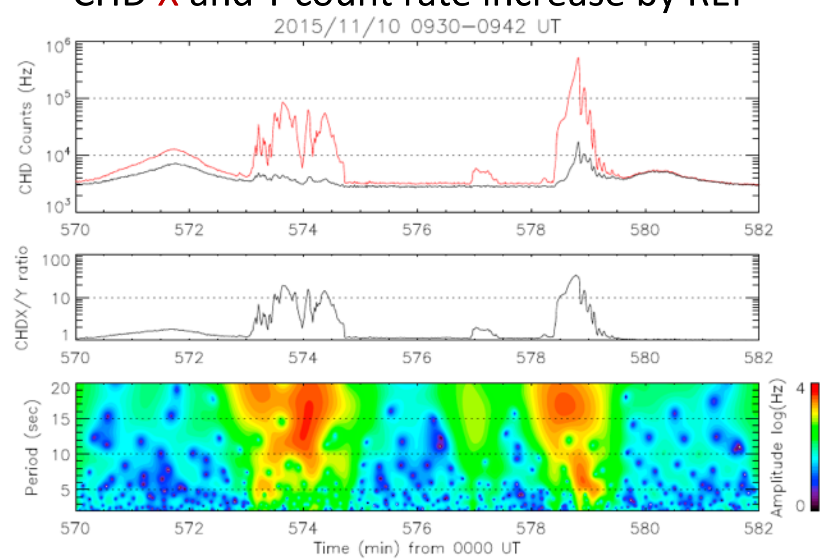

Summary and Future Prospects

- CALET was successfully launched on Aug. 19th, 2015, and the detector is being very stable for observation since Oct. 13th, 2015.

- As of Nov. 30th, 2017, total observation time is 780 days with live time fraction to total time to close 84%. Nearly 508 million events are collected with high energy (>10 GeV) trigger.

- Careful calibrations have been adopted by using "MIP" signals of the non-interacting p & He events, and the linearity in the energy measurements up to 10^6 MIPs is established by using observed events.

- Preliminary analysis of nuclei, total electrons and gamma-rays have successfully been carried out to obtain the energy spectra in the energy range;
  Protons: 55 GeV~22 TeV, C-Fe: 300 GeV~100 TeV, Total electrons: 10 GeV~4.5 TeV.

- Preliminary analysis of UH cosmic-ray flux are done up to Z=40.

- CALET's CGBM detected nearly 60 GRBs (~20 % short GRB among them) per year in the energy range of 7 keV-20 MeV, as expected. Follow-up observations of the GW events were carried out. (Not reported in this talk)

- The so far excellent performance of CALET and the outstanding quality of the data suggests that a 5-year observation period is likely to provide a wealth of new interesting results.

Examples of Electron Candidates in TeV Region

Energy: 3.62 TeV (θ=26.5°)

Energy: 6.75 TeV (θ=32.3°)

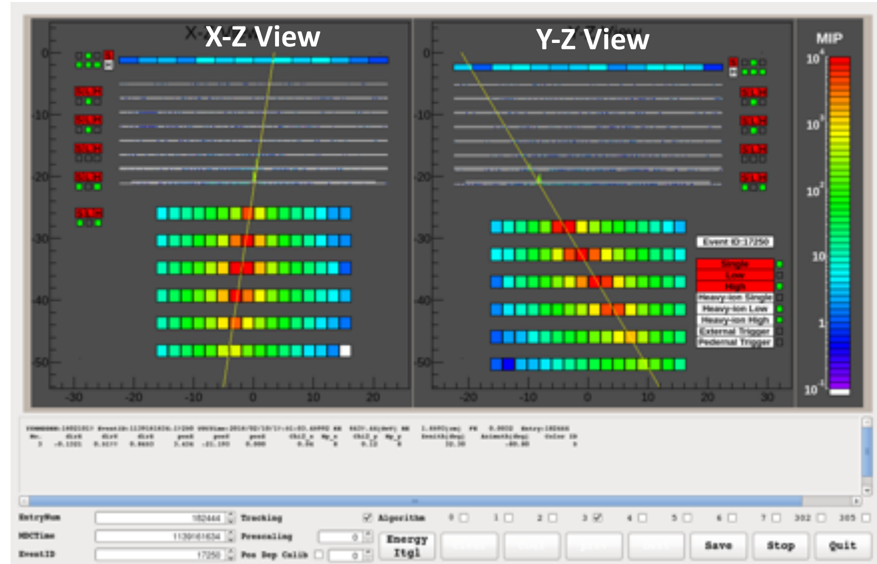

Longitudinal development of shower particles in IMC and TASC with fit of EM shower

IMC: Pre-shower

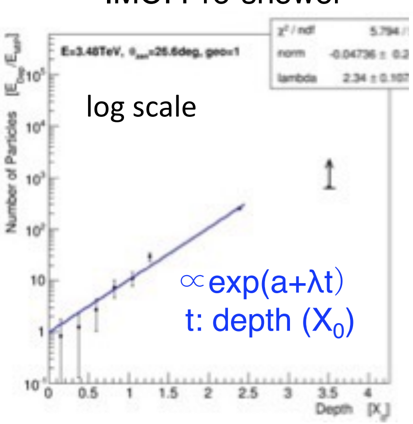

TASC

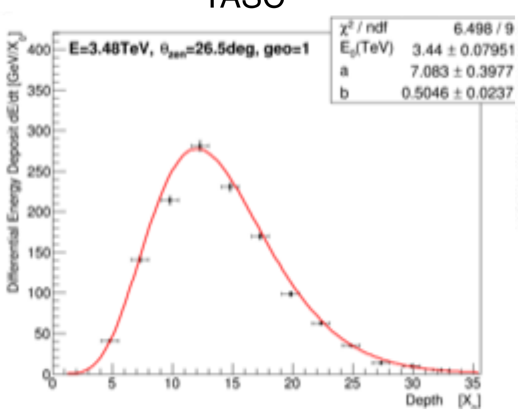

IMC: Pre-shower

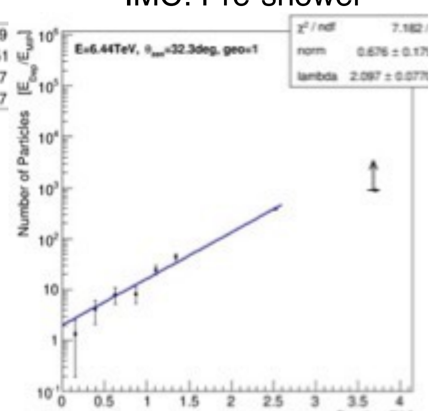

TASC